Results of the Static Pile Load Tests.

Jan Maertens, Jan Maertens bvba & Catholic University of Leuven (KUL)
Noël Huybrechts, Belgian Building Research Institute (WTCB-CSTC-BBRI)

Abstract

It is the objective of this report to compare the calculated and measured pile bearing capacities from 10 ground displacement screw piles and 2 driven prefabricated piles, which have been statically tested upon failure at the Sint-Katelijne-Waver test site, where the subsoil exists out of stiff fissured overconsolidated Tertiary Boom clay.
The calculations will be based on the semi-empirical methods used in Belgium to deduce the pile bearing capacity from cone penetration tests (CPT).
Out of this analysis the authors will suggest installation coefficients for this specific test site, which can be integrated in the work of the Belgian NAD-commission for the Eurocode 7.

1. Introduction

At least 90 % of all pile design in Belgium is based on semi-empirical formulae, directly assessing both base and shaft resistance of compression piles from CPT data in the natural ground conditions (i.e. before pile installation). The method itself is basicly the same for most common pile types (displacement as well as bored piles) and for non-cohesive and cohesive soils, but the formulae include pile and soil depending empirical factors, which are deduced from calibration with pile load test results.
Until recently, a lack of uniform calibration tests on soil displacement screw piles, in order to determine the installation factors, could be observed, and this in spite of the frequent use of these pile types. For that reason a research project adressing soil displacement screw piles has been inititated. The project took place in collaboration with five Belgian companies which install these pile types. Twelve static pile load tests have been executed on 5 types of screw piles and on driven prefabricated piles, installed in O.C. Tertiary Boom clay.
This report compares the test results with the results of the semi-empirical calculation methods used in Belgium. For that reason some reasonable assumptions have been made adressing pile failure criterion, calculation methods, type of CPT, etc. Several of these assumptions still have to be discussed in the EC7 working group for the Belgian National Application Document, which for the time being is still under draft. As long as no final decisions have been made so far, these assumptions as well as reference to the NAD contained in this report have to be considered as tentative.

2. Calculation of the pile bearing capacity

Preliminary remark

The Belgian practice adressing design of axially loaded piles has extensively been described in (Holeyman and al., 1997), of which several parts have been integrated in this chapter.

The pile bearing capacity exists out of two components: the pile base resistance and the shaft friction. Both components can be deduced from Cone Penetration Tests, by means of semi-empirical calculation methods.

The ultimate unit pile base resistance will be determined by the De Beer method (De Beer, 1971), starting from cone penetration tests with electrical E1-cone (CPT-E1).
The ultimate shaft friction will be determined, either from the total side friction as measured in discontinuous executed cone pentration tests with M1-cone (CPT-M1)., or as a fraction of the cone resistance out of CPT-E1.

Notice that, when calculations are based on cone resistance values (q_c), CPT-E1 are considered as reference. This is a very important assumption because, especially in O.C. Tertiary clays, variations between q_c values obtained from cone penetration tests with a mechanical cone type (CPT-M) and q_c values from CPT-E can be important.
The total side friction (Q_{st}) does not appear to significantly depend on the CPT method. More details about this subject are given in an other lecture presented at this symposium (P. Mengé, 2001).

Basic formulae
The pile ultimate base resistance R_{bu} is deduced from the CPT data by :

$$R_{bu} = \beta.\alpha_b.\varepsilon_b.q_{bu}^{(m)}.A_b$$

with :

β :a shape factor introduced for non-circular nor square-shaped bases;
β = (1 + 0.3(B/L))/1.3 with B = width and L = length of a rectangular base;

α_b :an empirical factor taking into account the method of installation of the pile and soil type;

ε_b :a parameter referring to the scale dependant soil shear strength characteristics (e.g. in case of fissured soil; see further)

$q_{bu}^{(m)}$:ultimate unit pile base resistance derived from the CPT results in the natural ground conditions by the De Beer method (see further)

A_b :the nominal pile base cross-sectional area.

Estimation of the ultimate shaft friction R_{su} is based on one of the following CPT values : the total side friction Q_{st} from the CPT or the cone resistance q_c (from CPT-E1).
The total pile shaft resistance R_{su} can be directly evaluated by proportioning the pile shaft resistance to the CPT total side friction increment ΔQ_{st} in the relevant shaft bearing layer(s) :

$$R_{su} = \frac{X_s}{\pi d}.\xi_f.\Delta Q_{st} \quad \text{or} \quad = \frac{X_s}{\pi d}.\sum \xi_{fi}.\Delta Q_{sti}$$

with :

ξ_f an overall empirical factor (=α_s . β_s . ε_s) introducing the effects of pile installation method (α_S), of the nature of the pile shaft material and roughness (β_S) and soil structure scale effects (ε_S);

X_s and πd :the perimeter of the pile shaft and of the sounding rod, respectively.

Although the use of the ΔQ_{st} based method was, and still is, common in pile design practice, the tendency exists to replace it by the method based on q_c-values. The reason being the possible imprecise measurement of Q_{st}, which can be strongly dependend on the execution of the CPT itself. As this method has been commonly

used, it has also been applied in the case of the piles tested at the Sint-Katelijne-Waver test site.

The pile shaft friction can also be evaluated from a semi-empirical correlation between the ultimate unit shaft friction q_{su} and the cone resistance values q_c :

$q_{su} = \eta_p . q_c$ or further detailed as: $q_{su} = \xi_f . \eta_p^* . q_c$

and thus :

$R_{su} = X_s \sum H_i . \eta_{pi} . q_{ci} = X_s \sum H_i . \xi_{fi} . \eta_{pi}^* . q_{ci}$

wherein η_p = an overall empirical factor depending on both soil and pile type. For clarity, the correlation $\eta_p = q_c/q_{su}$ can be split into (1) a pure soil parameter η_p^* equal to the ratio of q_c and the average unit side friction $q_{bu}^{(m)}$, and (2) a pile/soil dependant empirical factor ξ_f (as defined already before).

Calculation of $q_{bu}^{(m)}$: the De Beer method

One fundamental aspect of the Belgian pile design is the introduction of the so-called "scale effect" for the pile base resistance. The scale effect aims to take into account that the base resistance of a pile is defined by the failure pattern, which extends over a certain height below and above the pile toe, this height being related to the pile base diameter. The approach aims at transforming the CPT diagram (generally obtained with a 3.6 cm diameter cone) into the CPT diagram that would be obtained with a sounding rod having a diameter equal to that of the pile base.

While in foreign countries this scale effect is calculated by rather simple mathematical approaches (smoothing and averageing the q_C-values over a certain range) such as (France and The Netherlands), a more analytical method has been developed in Belgium in the 70's by De Beer (1971) and then been widely introduced in the Belgian design practice. It has been observed that the method aims to predict the limit load ($Q_{0.025Db}$) near the upper and lower boundaries of the bearing layer but provides the conventional rupture load ($Q_{0.10Db}$) at large depths in that layer.

The De Beer method is based on a thorough application of the principles of the scale effect, when transitioning from a soft to a hard soil layer as shown in Figure 1. This application of the scale effect is done in 4 steps, designated by the terms (a) homogeneous values, (b) descending or downward values, (c) upward values and (d) mixed or blended values. These final mixed values $q_{bu}^{(m)}$ are the basis values for the further base resistance calculation of the pile.

To demonstrate the procedure, step by step results of a De Beer calculation are given in figure 2 for a simplified soil profile.

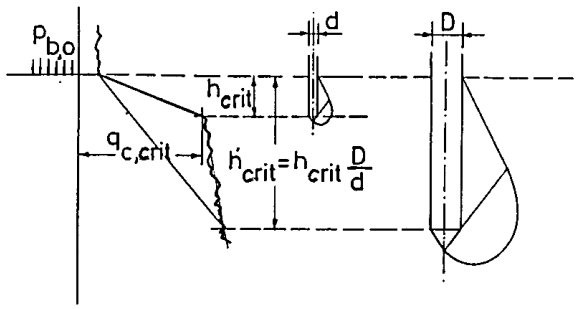

Figure 1- The scale effect principle

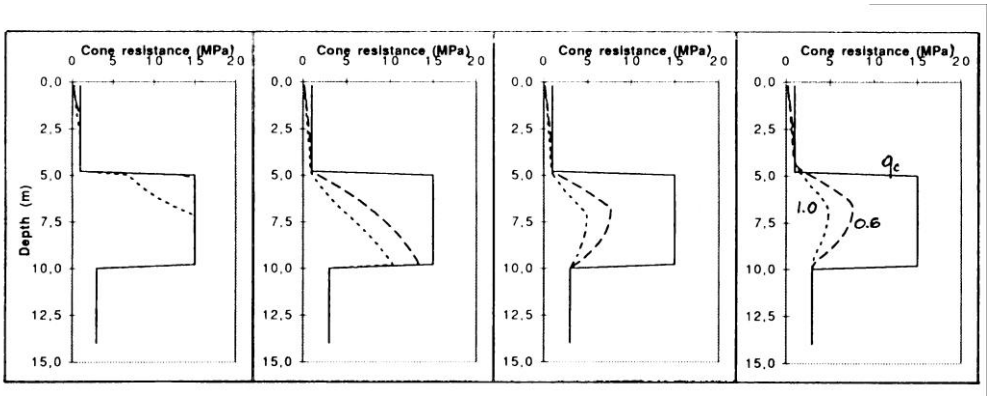

Figure 2 – Step by step illustration of De Beer procedure: (a) homogeneous values, (b) downward values, (c) upward values and (d) blended values; for a 0.6 and 1.0m diameter base, respectively.

Application of the the design formulae for the piles at Sint-Katelijne-Waver

For all the piles installed at the test site $\beta = 1$.

The ε_b parameter has been introduced to take into account the scale effect of the size of the failure mechanism of a pile base relative to the failure mechanism of the CPT cone, as recognized in the stiff fissured OC Boom clay (De Beer and al., 1977), but also in London clay. Although size dependent shear resistance might also exist in other soil types, this phenomenon has been explicitely introduced only in stiff OC clay, where, one applies in Belgium : $0.476 \leq \varepsilon_b \approx 1 - 0.01(D_b/d - 1)$

The shaft friction for the pile will be considered between a depth of 1.1 meters (excavation around the pile head) until the pile base level (±7.5 m or ±11.7 m depth). For the overall considered depth one constant factor ξ_f and one constant factor η_p will be assumed (in fact η_p is function of the cone resistance q_c, which varies in this case between 1.6 and 3 Mpa over the full pile depth range).

In this way the design formulae are are simplified to

$$R_{bu} = \alpha_b . \varepsilon_b . q_{bu}^{(m)} . A_b$$

$$R_{su} = \frac{X_s}{\pi d} . \xi_f . \Delta Q_{st}$$

$$R_{su} = \eta_p . X_s . \sum H_i . q_{ci}$$

The total bearing capacity of the pile is then:

$$R_{cu} = R_{bu} + R_{su}$$

The nominal diameters for the pile base (D_b) and shaft (D_s), as well as the pile base depths that have been used for the calculation of the bearing capacity are summarised in the table 1. D_b, D_s, as well as the definition of the pile base level have been specified by the contractors of each pile type before the execution of the pile load tests.

Pile number	Pile type	D_b (m)	D_s (m)	Pile base depth (m) [(1)]
A1	Driven Prefabr. 35x35	0.395	0.395	-7.39
A2	Fundex 38/45	0.450	0.380	-7,38
A3	Fundex 38/45	0.450	0.380	-11,50
A4	Driven Prefabr. 35x35	0.395	0.395	-11,58
B1	De Waal 41/41	0.410	0.410	-7,53
B2	De Waal 41/41	0.410	0.410	-11,73
B3	Olivier 36/51	0.510	0.510	-11,68
B4	Olivier 36/51	0.510	0.510	-7,43
C1	Omega 41/41	0.410	0.410	-7,67
C2	Omega 41/41	0.410	0.410	-11,83
C3	Atlas 36/51	0.510	0.510	-11,76
C4	Atlas 36/51	0.510	0.510	-7,72

(1) Measured pile base depth relative to original soil surface level, and related to the definition of the pile base level.

Table 1 – diameters D_b and D_s and pile base depths for calculation of the bearing capacity of the static tested piles

Reference calculations were made based on the individual CPT and average data. Only the known installation factors β and ε_b have been applied. The installation factors α_b, ξ_f and η_p have not been applied, as it is the aim to determine them when comparing the reference calculation results with the measurements.

Calculations based on individual CPT (table 2)

For the pile base, $q_{bu}^{(m)}$ is determined by applying the De Beer method (De Beer,E. 1971-1972) on the electrical CPT data in the axis of the pile (notice that q_c-data each 0.2 meter depth have to be considered). On the one hand the shaft friction is deduced from the CPT-M1 total side friction ΔQ_{st} measurement. Calculations have been made based on the M1 at each side (at 2-m distance) of the pile, indicated with the indices $^{(1)}$ and $^{(2)}$ in table 2. The average of these two values is given by the index $^{(av.)}$. On the other hand the shaft friction is deduced from the cone resistance of the CPT-E1 in the axis of the pile following $Q_{su} = X_s.\sum H_i.q_{ci}$.

Calculations based on average data (table 3)

The unit pile base resistance $q_{bu}^{(m)}$ for a specific pile is calculated with the De Beer method for each CPT-E1 in the static test field (q_c values each 0.2 m). Herefrom the average value is determined and taken into account.

For the shaft friction of a specific pile, calculations have been made for each CPT in the static test field (CPT-M1 when friction deduced from ΔQ_{st} and CPT-E1 when friction deduced from cone resistance q_c). From these values the average is determined and taken into account. The results are summarised in the table 3.

Pile	ε_b	$q_{bu}^{(m)}.A_b$ [kN]	$\varepsilon_b.q_{bu}^{(m)}.A_b$ [kN]	$(Xs/\pi d)\Delta Q_{st}$ [kN]			$X_s\sum H_i q_{ci}$ [kN]
				$(Xs/\pi d)\Delta Q_{st}^{(1)}$	$(Xs/\pi d)\Delta Q_{st}^{(2)}$	$(Xs/\pi d)\Delta Q_{st}^{(av.)}$	
A1	0.90	263.0	**236.7**	655.2	564.8	**610.0**	**13019**
A2	0.88	363.2	**319.6**	598.0	534.2	**566.1**	**12038**
A3	0.88	457.7	**402.8**	1107.1	1107.0	**1107.1**	**28442**
A4	0.90	326.3	**293.7**	1171.2	1173.3	**1172.2**	**30079**
B1	0.90	295.1	**265.6**	541.4	601.2	**571.3**	**14923**
B2	0.90	305.0	**274.5**	1148.0	948.4	**1048.2**	**30547**
B3	0.87	536.7	**466.9**	1581.8	1465.2	**1523.5**	**37485**
B4	0.87	482.5	**419.8**	761.4	794.9	**805.0**	**19258**
C1	0.90	306.5	**275.9**	632.3	753.8	**693.0**	**16683**
C2	0.90	286.2	**257.6**	1349.9	1425.6	**1387.7**	**30423**
C3	0.87	527.0	**458.5**	1649.3	1550.5	**1599.9**	**39983**
C4	0.87	503.1	**437.7**	945.8	829.9	**887.9**	**21776**

Table 2 – Reference calculations $\varepsilon_b.q_{bu}^{(m)}.A_b$; $(X_s/\pi d)\Delta Q_{st}$ and $X_s.\sum H_i.q_{ci}$ based on individual CPT

Pile	ε_b	$q_{bu}^{(m)}.A_b$ [kN]	$\varepsilon_b.\ q_{bu}^{(m)}.A_b$ [kN]	$(X_s/\pi d)\Delta Q_{st}$ [kN]	$X_s.\sum H_i.q_{ci}$ [kN]
A1	0.90	264.9	**238.4**	**607.1**	**14652**
A2	0.88	341.7	**300.7**	**582.7**	**14096**
A3	0.88	405.9	**357.2**	**1115.7**	**27668**
A4	0.90	314.4	**283.0**	**1174.2**	**29002**
B1	0.90	285.5	**257.0**	**638.3**	**15637**
B2	0.90	340.9	**306.8**	**1248.7**	**30565**
B3	0.87	521.7	**453.9**	**1542.8**	**38020**
B4	0.87	436.6	**379.8**	**791.6**	**19155**
C1	0.90	285.9	**257.3**	**648.2**	**16213**
C2	0.90	342.1	**307.9**	**1270.4**	**30944**
C3	0.87	523.2	**455.2**	**1665.5**	**38491**
C4	0.87	438.7	**381.7**	**815.3**	**20286**

Table 3 – Reference calculations $\varepsilon_b.q_{bu}^{(m)}.A_b$; $(X_s/\pi d)\Delta Q_{st}$ and $X_s.\sum H_i.q_{ci}$ based on average data

3. Static pile load tests at Sint-Katelijne-Waver : Test procedure and Results

The calculated reference values of the bearing capacities $\varepsilon_b.q_{bu}^{(m)}.A_b$; $(X_s/\pi d)\Delta Q_{st}$ and $X_s.\sum H_i.q_{ci}$, as summarised in the tables 2 and 3 of the previous chapter, need to be compared with measured values of the pile bearing capacities R_{cu}, R_{bu} and R_{su}, in order to deduce the installation coefficients α_b, ξ_f, and η_p. These measured values can be deduced out of the full scale static load tests, which were executed on the 12 piles. It is important to consider that the determination of the measured bearing capacities depends upon the definition of a pile failure criterion. Furthermore, the followed load test procedure might influence the test results and as a consequence the measured bearing capacity values.

Test procedure

In accordance with the national advisory committee and taking into account the activities of the ERTC3 (European Regional Technical Committee 3 – piles) a test procedure for the static pile load tests was postulated. The maximum test load Q_{max} was determined before the test in order to provoke pile failure under this load (see

further). Figure 3 illustrates graphically the followed test procedure, which can be summaried as follows:

- Applying a preload stage of maximum 5% of Q_{max} in order to check the measurement equipment and the centricity of the applied force;
- Executing 10 constant loading steps with equal ΔQ until Q_{max} is achieved;
- Holding each load step constant during 60 minutes;
- No intermediate unloading cycles during the static load test;
- When the pile head settlement has reached a value of 25 mm, the next load steps will be taken smaller ($\Delta Q/2$), in order to refine this area of the pile load-settlement curve;
- Failure of the pile under constant pile head velocity of 0.6 à 0.8 mm/min
- Executing the load test until a pile head settlement $s_0 \geq 15\% \varnothing_{base}$ is reached
- Unloading in 4 steps of 10 minutes each, except for total unloading (minimum 30 minutes).

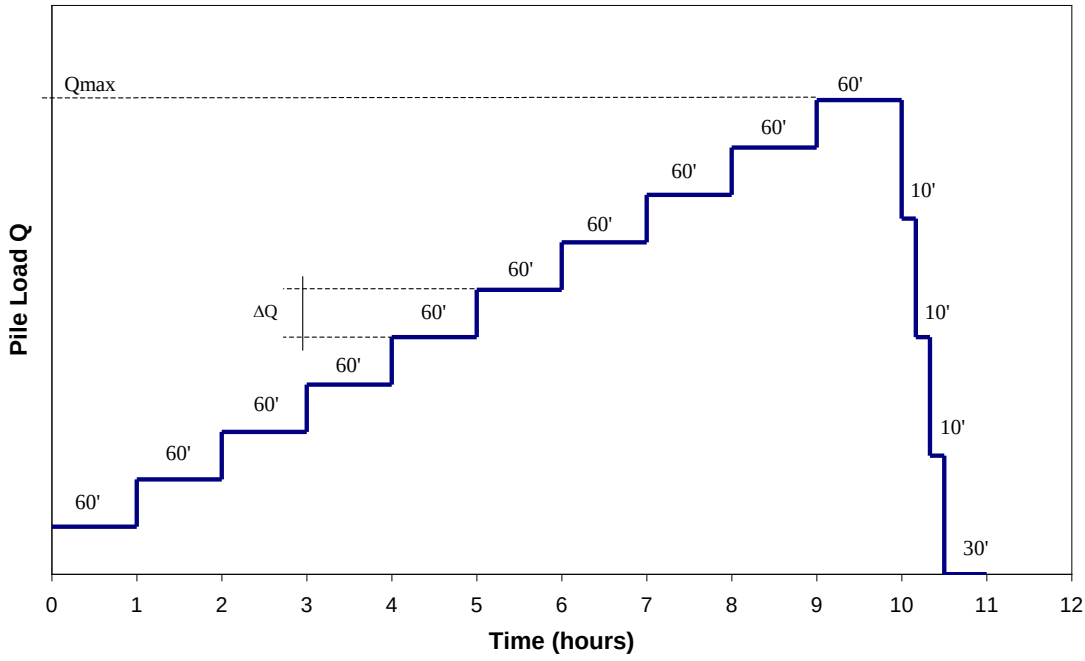

Figure 3 – Test procedure static pile load test

Remarks

For each pile, Q_{max} was determined based on the calculation rules applied in Belgium (see chapter 2)**,** taking into account installation coefficients from literature data adressing static pile load tests on displacement piles in OC clay, among others (De Beer and al., 1977) and (De Cock F. and al., 1993). Based on these data, a value of ΔQ was derived in order to obtain pile failure after 8 to10 equal load steps. If for a certain pile type the number of load steps deviated too much, ΔQ was adapted for the second load test of that pile type, taking into account the results of the first load test.

As the pile head velocity might influence the executed pile load in cohesive soils, it was assumed that pile failure should be controlled, by enhancing a constant pile head velocity. A value of 0.6 to 0.8 mm/min during pile failure was postulated based on literature data for CRP tests (Constant Rate of Penetration tests), among others in (ISSMFE 1985), in the American Standard (ASTM D1143-81, 1994) and in the

British Standard (BSI, 1986). These controlled constant pile velocity during failure was enhanced for all piles except the driven prefabricated piles.

Test results

Following the postulated load test procedure, the 12 static pile load tests have been executed in the period between August 30th and Octobre 12th 1999. All the piles have been tested 3 to 3.5 months after installation, to exclude discussion about the influence of the time effect (reconsolidation of the clay) on the results of the different piles.

For each pile the test results are graphically represented in Annex A.
In annex A the a-figures illustrate the load-settlement diagram together with a plot showing the increase of settlement $\Delta s_{0\text{-}i,30}$, during the last 30 minutes of a load step i versus the pile load Q (creep curve).
For the load-settlement diagram, different symbols have been used :

- ◆ = final pile head settlement under a constant loading, unloading or reloading step;
- ● = pile head settlement during failure of the pile under a constant pile head velocity;
- ■ = pile head settlement during failure of the pile under a non constant pile head velocity

A dashed type of line has been used to connect the second last complete (= 60') load step (indicated with the symbol ◆) with the last non complete load step during which failure occures (indicated with symbols ● or ■), as well as for the connections between the points illustrating the failure of the pile.

On the creep curve two straigt lines have been drawn, in order to deduce the creep load Q_c, according to the prescriptions of the ISSMFE (1985). Mostly, a creep curve shows two linear parts, of which the intersection is defined as the creep load Q_c. However, several creep curves of the piles tested at Sint-Katelijne-Waver show more than two linear parts, making interpretation difficult. The existance of more than two linear parts in creep curves and the corresponding interpretation difficulties are described in(Jezequel J. and al., 1970). For the tests at Sint-Katelijne-Waver Q_c has arbitrary been deduced from the intersection of two linear parts: one line through the last two points of the creep curve and the other line as linear approach through the first series of points.

The b-figures in annex A illustrate the time-settlement results for the different (complete) load steps, with the time on a logarithmic scale.

Remarks

Pile C3 exhibits an unusually high peak, with the load increasing very rapidly up to about 2300 kN within a 6 to 20 mm settlement range. This was due to a problem in the pressure regulation of the hydraulic jack. After reaching a settlement of 6 mm, the pile started to settle at a rate of penetration of approximately 48 mm/min. This explains that the peak capacity of the SLT (about 2300 kN) is an overestimate of the pile ultimate static bearing capacity. In the absence of that regulation problem, the peak would have been reached under a load of approximately 1650 kN. This test evidences the influence of the rate of penetration on the assessment of piles ultimate bearing capacities. After total unloading the pile C3, reloading has taken place in

steps of 10 minutes each until the point were the regulation problem occurred. From this point on the load test was continued as planned, finally reaching a peak of 1736 kN. Load and settlement values adressing pile C3 (see further) have been based on this reloading cycle.

4. Analysis & interpretation

Deduced load and settlement data

In the table 4, pile loads according to different criteria have been summarised for the different piles. These load values are derived from the a-figures in Annex A, and correspond with the maximum achieved test load Q_{max}, with an absolute pile head settlement s_0 of 25 mm (Q_{25mm}) , with a relative s_0 of 10%D_b ($Q_{0.10Db}$) and 15%D_b ($Q_{0.15Db}$) and with the creep load Q_c.

Pile	Q_{max} [kN]	Q_{25mm} [kN]	$Q_{0.10Db}$ [kN]	$Q_{0.15Db}$ [kN]	Q_c [kN]
A1	969	916	832	810	780
A2	809	797	786	761	720
A3	1294	1283	1216	1171	1110
A4	1653	1531	1364	1324	1240
B1	788	779	743	712	625
B2	1304	1298	1258	1224	940
B3	1844	1750	1722	1601	1590
B4	1189	1150	1134	1004	1030
C1	735	733	719	707	600
C2	1304	1300	1263	1232	960
C3	1736	1725	1637	1538	1480 max
C4	1014	990	917	897	740

Table 4 – Q_{max}, Q_{25mm}, $Q_{0.10Db}$, $Q_{0.15Db}$ and Q_c for the different piles

In table 5 one can find a **"nuttige last" (allowable load??)** Q_N deduced from the creep load following to $Q_N = 0.8Q_c$, the relation $Q_{0.10Db}/Q_N$ and the values of the pile head settlement s_0 corresponding with Q_N, deduced from the load settlement diagram. **(Hier verwijzen naar Franse methode /LCPC??)**

Finally in table 6 one can find the **"nuttige last" (allowable load??)** Q_N deduced from the creep load ($0.8Q_c$) as already shown in the previous table, and **"nuttige lasten" (allowable loads??)** Q_N deduced from the conventional rupture load $Q_{0.10Db}$ by dividing it with 1.7 and 2 respectively. The pile head settlement corresponding with each defined Q_N value is also presented in the table 6. These factors 1.7 and 2 are safety factors which are applied in Tertiary stiff clays on the calculations of ultimate shaft friction (R_{su}) and the pile base resistance (R_{bu}) respectively (deterministic calculation method which was, and still is, common in current practice in Belgium. However, by the introduction of the EC7 these deterministic approach with global safety factors will be replaced by the semi-probalistic calculation method using partial safety factors).

(NA TE KIJKEN : in de eerste draft van een document van Afdeling Geotechniek worden waarden van 2.1 en 1.8 gebruikt)

Pile	$Q_N = 0.8Q_c$ [kN]	$Q_{0.10Db}/Q_N$ [-]	s_o [mm]
A1	624	1.33	2.44
A2	576	1.36	3.82
A3	888	1.37	3.17
A4	992	1.38	2.93
B1	501	1.48	3.51
B2	752	1.67	2.55
B3	1272	1.35	7.06
B4	824	1.38	6.79
C1	480	1.50	2.71
C2	768	1.64	2.31
C3	1184_{max}	1.38	4.53_{max}
C4	592	1.55	2.85

Table 5 – **"Nuttige last**" $Q_N = 0.8Q_c$, relation with $Q_{0.10Db}$ and corresponding s_0

Pile	$Q_N = 0.8Q_c$ [kN]	s_o [mm]	$Q_N = Q_{0.10Db}/1.7$ [kN]	s_o [mm]	$Q_N = Q_{0.10Db}/2$ [kN]	s_o [mm]
A1	624	2.44	489	1.50	416	1.13
A2	576	3.82	462	2.28	393	1.70
A3	888	3.17	715	2.03	608	1.57
A4	992	2.93	802	2.17	682	1.78
B1	501	3.51	437	2.43	372	1.66
B2	752	2.55	740	2.47	629	1.86
B3	1272	7.06	1013	4.24	861	3.25
B4	824	6.79	667	3.88	567	2.64
C1	480	2.71	423	2.09	360	1.64
C2	768	2.31	743	2.20	632	1.73
C3	1184_{max}	4.53_{max}	963	3.24	819	2.57
C4	592	2.85	539	2.33	459	1.74

Table 6 – **"Nuttige last"** Q_N following different **(deterministic)** methods and corresponding s_0

Remarks

When it is supposed that the **"nuttige last" (allowable load??)** $Q_N = \min\left[0.8Q_c\,;\,\frac{Q(10\%D_b)}{1.7\text{ of }2}\right]$, then it is obvious in this case that the values deduced from the conventional rupture load $Q_{0.10Db}$ are determinant for all piles.

?????

Out of table 6, it seems also that the settlement of the piles B3 and B4 acording to the Q_N values are somewhat higher than the settlements of the other piles, although its bearing capacities can be found at the higher limit of the bearing capacity range from the group of screw piles (see further)

?????

Separated pile base resistance and shaft friction : coefficients α_b, η_p and ξ_f

In order to deduce the empirical factors, the calculated reference values (chapter 2) need to be compared with the measured values of the pile bearing capacity. We will consider as failure criterion the conventional rupture load, i.e. the measured pile load according to a settlement of 10% of D_b, or $R_{cu,measured} = Q_{0.10Db}$

Moreover, to determine the separate installation factors for base and shaft α_b, ξ_f, and η_p, the total measured pile bearing capacity ($R_{cu,measured}$) needs to be separated in pile base resistance and shaft friction ($R_{bu,measured}$ and $R_{su,measured}$).

In order to determine these separated values the piles have been instrumented with a retrievable extensometer system, with which the pile deformations have been measured at different depths (ecxept for the piles A1, A4, and B3). More details of this measurement system and some results are given in an other lecture presented at this symposium (N. Huybrechts, 2001).

When these deformation measurements are multiplied with the pile material EA-factor (modulus of elasticity x pile section) the load distribution can be obtained.

From the extensometer measurements installation coefficients for the screw piles could be deduced in the following range:

α_b :0.60 to 0.95

ξ_f : 0.75 to 1.01

η_p :0.030 to 0.042

Furthermore it was expected that the difference of the measured total bearing capacity of the short versus the long pile of each type would give an approach of the separated installation factors for pile base and shaft, and this by solving a set of two equations with two unknown variables. Hereby it has been assumed that the installation factors for both the short and the long pile are the same, and that the η_p-factor is a constant factor over the full pile depth (in fact η_p is function of the cone resistance q_c, which varies in this case between 1.6 and 3 Mpa)

When the shaft friction is calculated from the total side friction ΔQ_{st} out of CPT-M1 the set of equations becomes (solving results in values for α_b and ξ_f):

$$Q_{0.10Db,short} = \varepsilon_b.\alpha_b.A_b.q_{bu}{}^{(m)}{}_{,short} + \xi_f.(D_s/d).\Delta Q_{st,short}$$

$$Q_{0.10Db,long} = \varepsilon_b.\alpha_b.A_b.q_{bu}{}^{(m)}{}_{,long} + \xi_f.(D_s/d).\Delta Q_{st,long}$$

When the shaft friction is calculated from the cone resistance q_c out of CPT-E1 the set of equations becomes (solving results in values for α_b en η_p):

$$Q_{0.10Db,short} = \varepsilon_b.\alpha_b.A_b.q_{bu}{}^{(m)}{}_{,short} + \eta_p.\sum (H_i.\pi.D_s.q_{ci})_{short}$$

$$Q_{0.10Db,long} = \varepsilon_b.\alpha_b.A_b.q_{bu}{}^{(m)}{}_{,long} + \eta_p.\sum (H_i.\pi.D_s.q_{ci})_{long}$$

With :

$Q_{0.10Db,short/long}$	:the measured total bearing capacity of the short/long pile (conventional rupture load)
$q_{bu}{}^{(m)}{}_{,short/long}$	:the calculated ultimate unit pile base resistance of the short/long pile determined with the De Beer method out the qc results of CPT-E1 .
$\Delta Q_{st,short/long}$	:the total side friction out of CPT-M1 over a depth corresponding with the short/long pile
$\sum (H_i.\pi.D_s.q_{ci})_{short/long}$	:shaft friction calculated out of the cone resistance qc of CPT-E1

A_b	:the nominal pile base cross-sectional area
D_s	:the nominale pile shaft diameter
d	:the diameter of the sounding rod (35.7 mm)
ε_b, α_b, ξ_f and η_p	:installation coefficients, with $\varepsilon_b = 1 - 0.01(D_b/d - 1)$

Notice that the calculated values in the equations ($q_{bu}^{(m)}$, ΔQ_{st}, en $\sum (H_i.\pi.D_s.q_{ci})$) can be determined based on individual CPT or based on the average data as specified in chapter 2.

When these set of equations are solved values of α_b, ξ_f, and η_p are obtained in the following range:

α_b :0.05 to 2.20

ξ_f : 0.57 to 1.07

η_p :0.017 to 0.040

Total pile bearing capacity – global coefficient

A global coefficient of the pile bearing capacity can be determined following the formula : global coefficient = $\dfrac{Q}{\varepsilon_b A_b q_{bu}^{(m)} + (\dfrac{D_s}{d})\Delta Q_{st}}$,with Q the measured pile head load. In the formula only the installation factor ε_b, which is assumed to be known, has been taken into account.

This global coefficient of the pile bearing capacity is graphically presented in the figures 4 and 5 for the whole course of the static test and this in function of the relative pile head settlement (s_0/D_b) expressed in percent.

Figure 4 illustrates the global coefficient of the different piles in the case that calculations have been made based on the individual CPT. Figure 5 gives this information in the case that calculations are based on average data.

Especially in this last case, the global coefficient curves of the screw piles show a quite similar course. When considering a pile head settlement $s_0 = 10\%.D_b$, a global coefficient of 0.77 à 0.97 is obtained for the screw piles. When the maximum value 0.97 is not taken into account (last load step for this tested pile was somewhat too big) the global coefficients are situated between 0.77 and 0.88.

For the driven prefabricated piles a global coeffcient of ± 0.95 can be estimated, corresponding to $s_0 = 10\%.D_b$.

These curves evolve to an asymptote. The global coefficients in accordance with great settelements can be estimated at 0.88 for the driven prefabricated piles and 0.74 for the ground displacement screw piles.

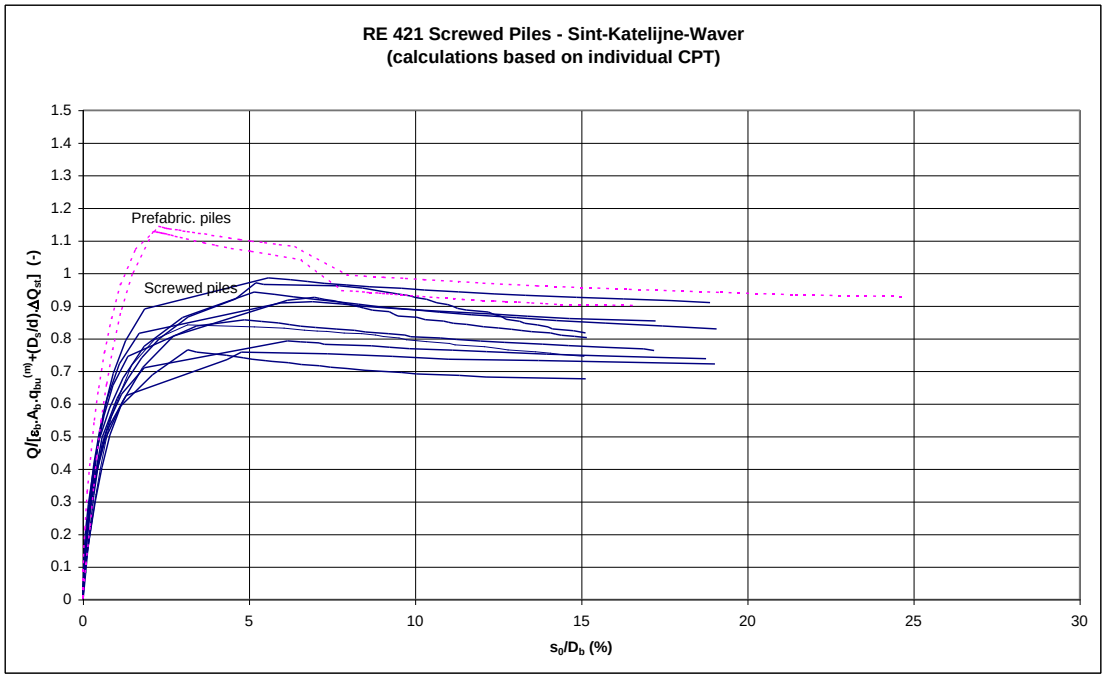

Figuur 4 – global coefficient – calculations based on individual CPT

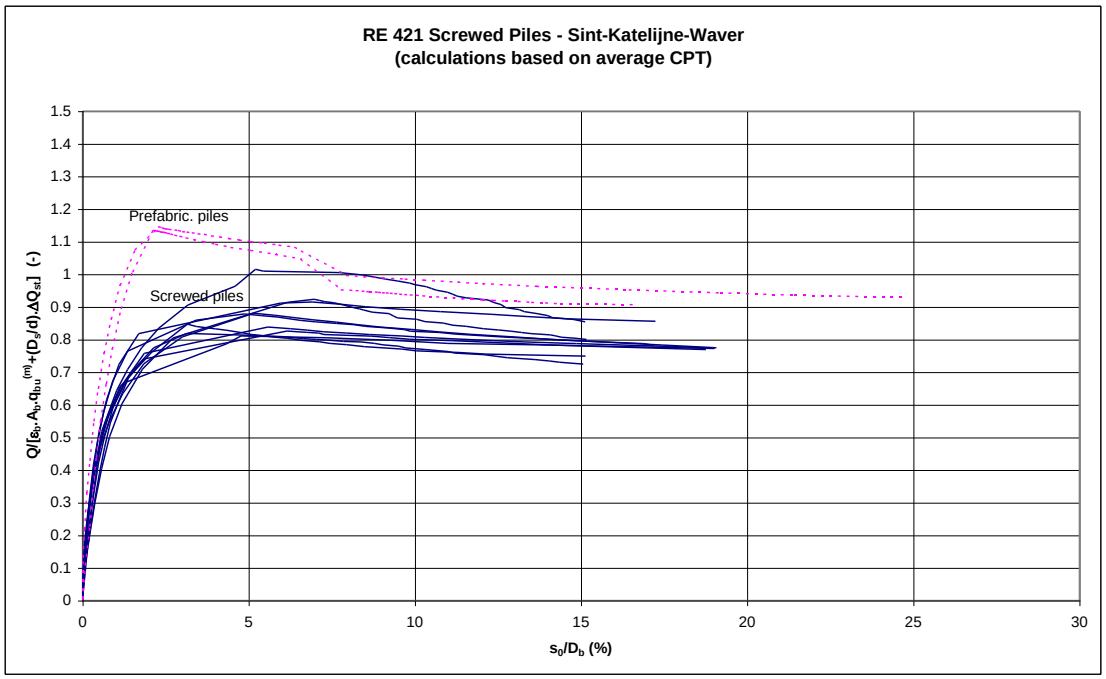

Figuur 5 – global coefficient – calculations based on average data

Discussion

1. Calculations based on average data give a more similar course of the global coefficient of the pile bearing capacity (measurement/calculation) for the different types of screw piles (see figure 5). This can be explained by the fact that the bearing capacity exist mainly out of shaft friction. Concerning the calculations of the shaft friction based on ΔQ_{st} values of the individual CPT-M1 at both sides of the pile, great variations can arise (see reference calculations in the table 2).

2. As it concerns friction piles, one can state that it has practically no influence on the determination of a global coefficient if the calculation of the base resistance is based on individual CPT or on average data.
3. The difference between the values of the shaft friction calculated out of the cone resistances from individual CPT-E1 or from the average data is rather limited.
4. The variation in the results of the separate installation factor α_b, ξ_f, and η_p deduced from extensometer measurements are rather great, especially for the α_b factor, which varies between 0.60 and 0.95 for the group of screw piles. This variation can partially be explained by variations on the applied EA values (modulus of elasticity x the section of the pile material), measurement corrections, heterogeneity of the fissured clay layer, etc. On the other hand different soil displacement characteristics at the pile base might exist between the different screw pile types. Also the variation of the results obtained from the solution of the set of equations (bearing capacity short pile versus long piles) show a very great variation, which can be explained by the high sensitivity of the solution of the set of equations for slight variations in the measured bearing capacity. In order to determine possible different soil displacement characteristics at the pile base for different types of screw piles, a test campaign at a end-bearing site is necessary.
5. The sensitivity of the shaft friction installation factors (ξ_f and η_p) for varitions of the pile base resistance was investigated. By increasing the α_b-factor from 0.5 to 1 (100%) , ξ_f and η_p decrease with ± 25 %.

5. Conclusions

The separate values for α_b, ξ_f, and η_p obtained from the static load tests show a rather great variation.

For the driven prefabricated piles, one can postulate the following values:
$\alpha_b = 1$, $\xi_f = 0.9$ en $\eta_p = 0.036$

Based on the available information for the soil displacement screw piles, it is not possible to formulate separate practicable values of α_b, ξ_f, and η_p to be applied for each pile type.

Based on the figure 5, one can note that for the screw piles the relation between the measured and calculated pile bearing capacity according to a settlement $s_0 = 10\%D_b$ amounts to a global value of 0.8. When the installation factors $\alpha_b = 0.8$, $\xi_f = 0.8$, and $\eta_p = 0.033$ are assumed, a reasonable and acceptable correspondence between the measured and calculated pile bearing capacity is obtained for all the different types of screw piles.
It is important to consider that these installation factors are valid, taking into account al the assumptions that have been made in this report:

- Calculations based on the cone resistance (q_c): CPT with electrical E1-cone
- Calculation method pile base : De Beer method (CPT E1)
- Nominal pile diameters following table 1.
- Pile base depth as defined by the contractor
- Test procedure as explained in chapter 3
- Failure criterion: conventional rupture load

Aknowledgements

nog aan te vullen eventueel

References

ASTM D1143-81, 1994. Annual Book of ASTM Standards section 4 – Volume 04.08. ASTM D1143-81 : Standard test method for piles under static axial compressive load.

BSI, 1986. British Standard code of practice BS 8004– Foundations; section 7 pile foundations.

De Beer; E., Lousberg, E., Wallays, M., Carpentier, R., De Jaeger,J. & Paquay, J. 1977. Bearing capacity of displacement piles in stiff fissured clays. I.R.S.I.A. – I.W.O.N.L., Comptes rendus de recherches – Verslagen over navorsingen, No 39, Brussel

De Beer,E. 1971-1972. Méthodes de déduction de la capacité portante d'un pieu à partir des résultats des essais de pénétration. *Annales des Travaux Publiques de Belgique,* No 4 (p.191-268), 5 (p321-353) & 6 (p 351-405), Bruxelles.

De Cock, F., Van Impe, W. & Peiffer, H. 1993. Atlas screw piles and tube screw piles in stiff Tertiary clays – Assesment of pile performance and pile capacity on basis of instrumented loading tests. Proceedings of the 2nd International Seminar on Deep Foundations on Bored and Auger Piles (BAP II), p. 577-586, Ghent.

Holeyman, A., Bauduin, C., Bottiau, M., Debacker, P., De Cock, F., Dupont, E., Hilde, J.L., Legrand, C., Huybrechts N., Mengé P., Simon G. 1997. Design of axially loaded piles – Belgian practice. *Proceedings of the ERTC3 seminar,* Brussels.

Huybrechts, N. 2001. Discussion of the installation techniques of the different types of screw piles & Test campaign at Sint-Katelijne-Waver : Organisation, Pursuit and Execution, *Proceedings of the Symposium on screw piles – installation coefficients in stiff clay,* March 15th 2001, Brussels

ISSMFE Subcommittee on Field and Laboratory testing. 1985. Axial Pile Loading Test-Part 1: Static Loading. *ASTM Geotechnical Testing Journal* , p.79-90.

Jezequel, J., Marchal, J. Essai statique de fondations profondes. Bulletin Liaison Labo Routiers Ponts et Chaussées, n° 44 – Mars-Avril 1970 – Réf. 843

Mengé, P. 2001. Soil investigation results at Sint-Katelijne-Waver, *Proceedings of the Symposium on screw piles – installation coefficients in stiff clay,* March 15th 2001, Brussels

ANNEX A

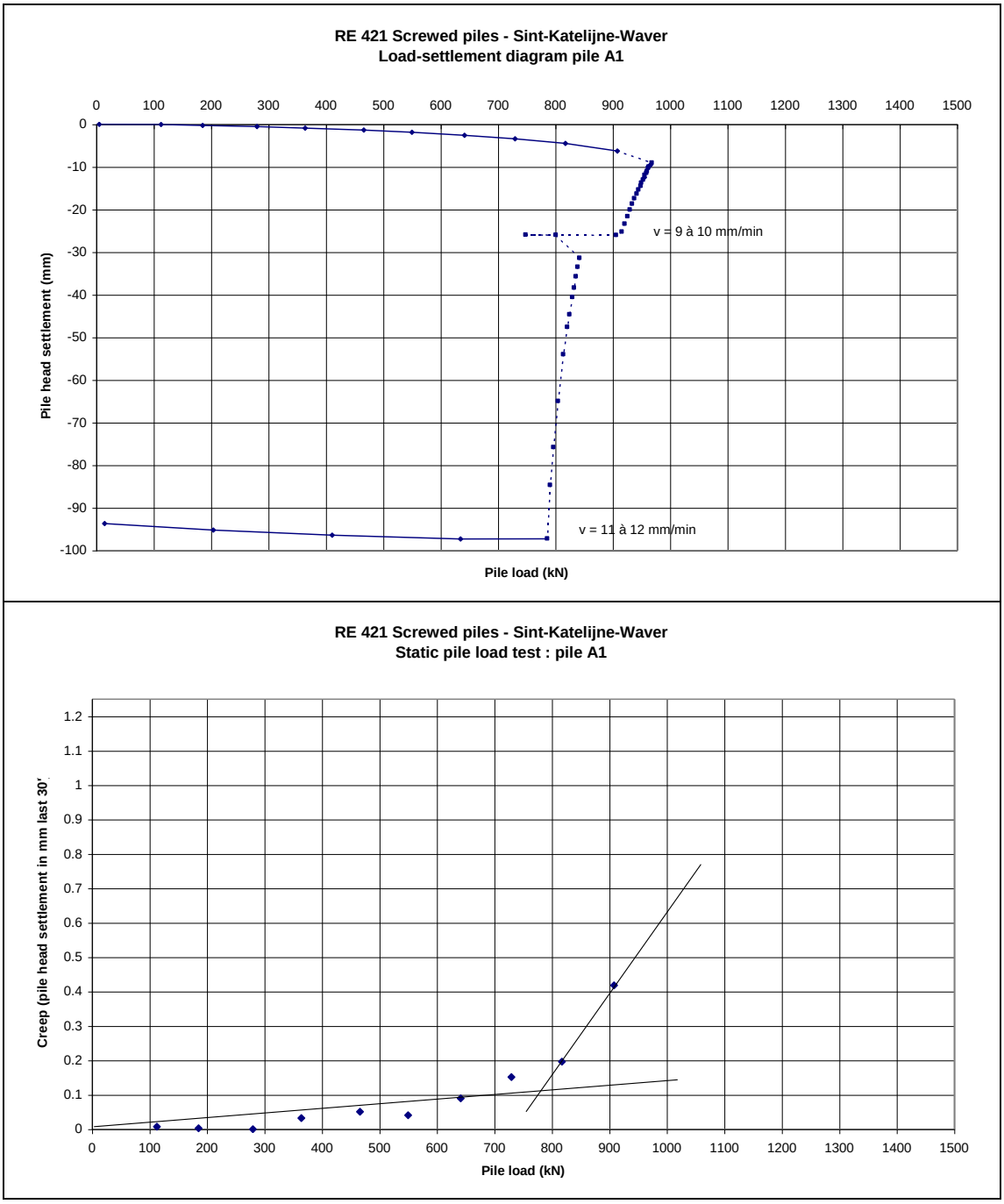

Figure A-1a – Load settlement diagram and creep curve (load vs. $\Delta s_{0\text{-}i,30'}$) driven prefabricated pile A1

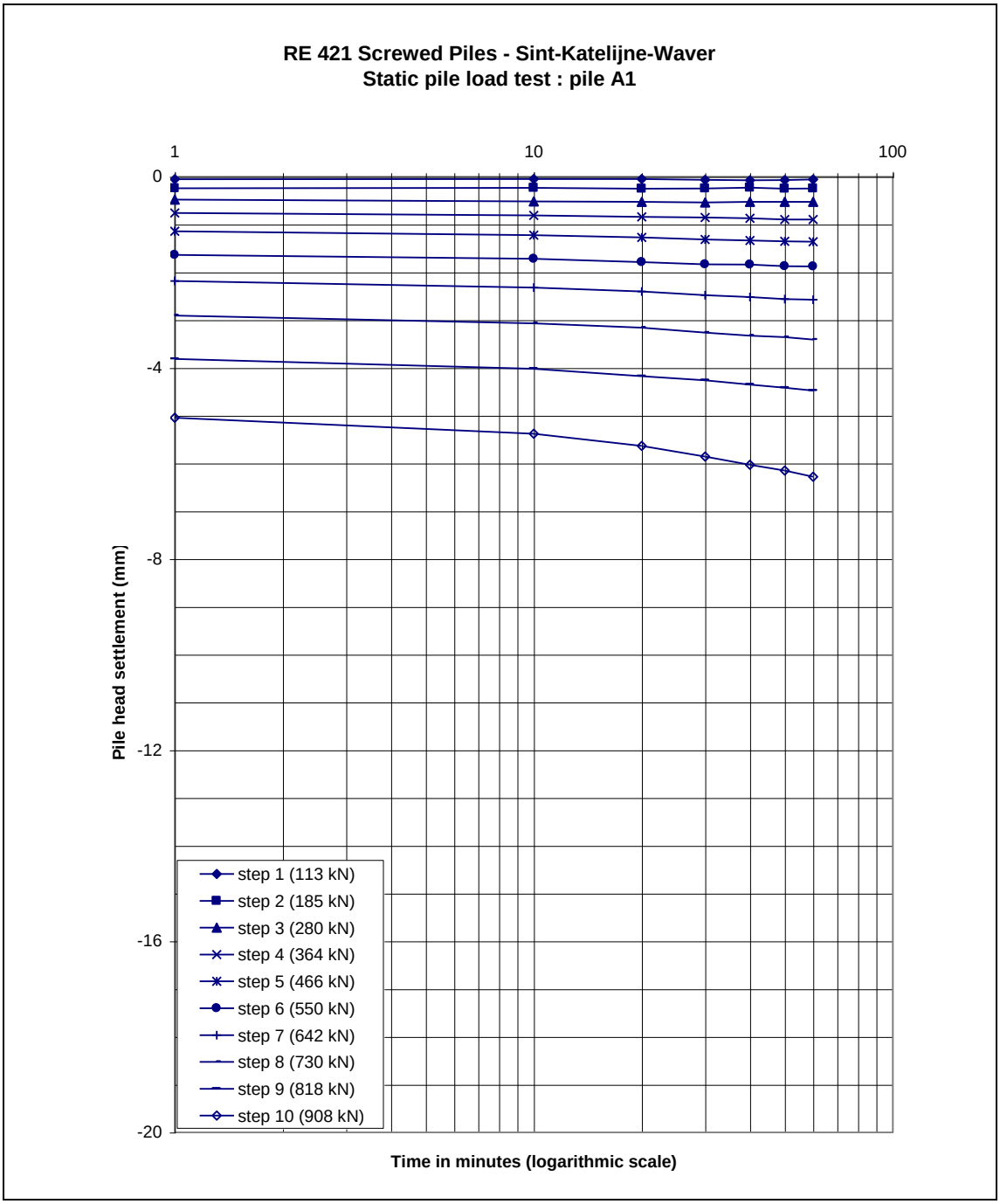

Figure A-1b – Time settlement results for the different (complete) load steps driven prefabricated pile A1

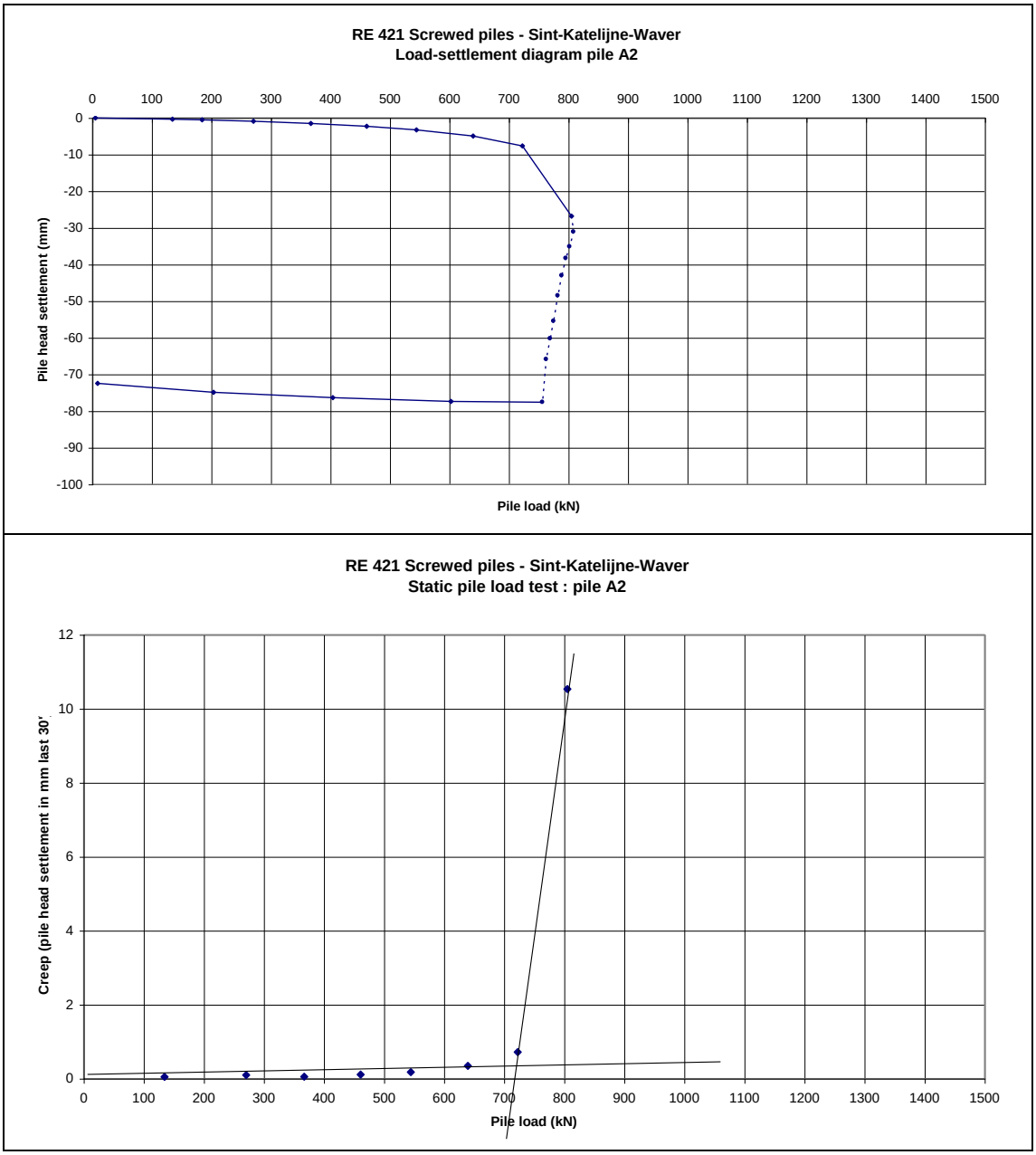

Figure A-2a – Load settlement diagram and creep curve (load vs. $\Delta s_{0\text{-}i,30'}$)
Fundex screw pile A2

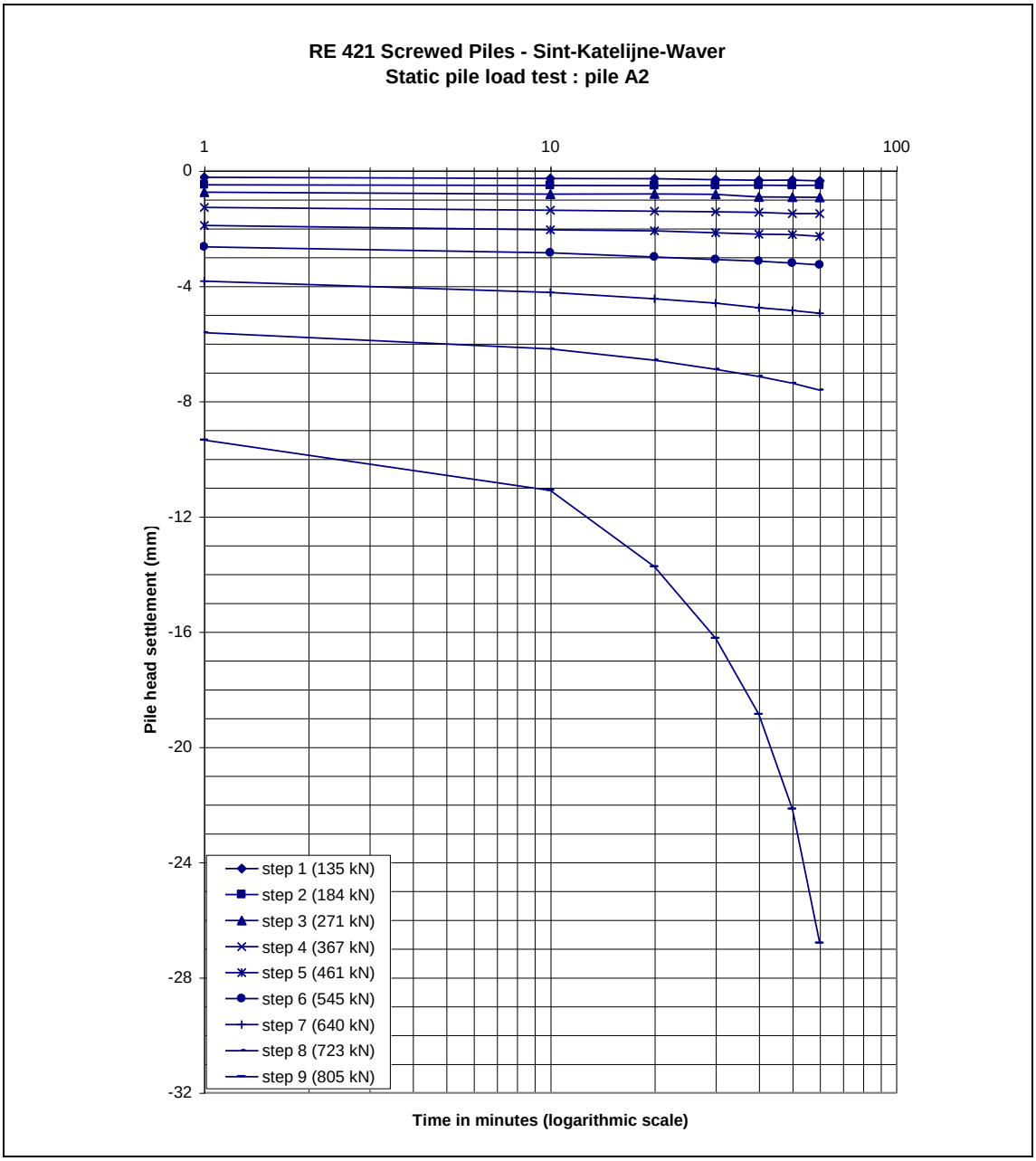

Figure A-2b – Time settlement results for the different (complete) load steps
Fundex screw pile A2

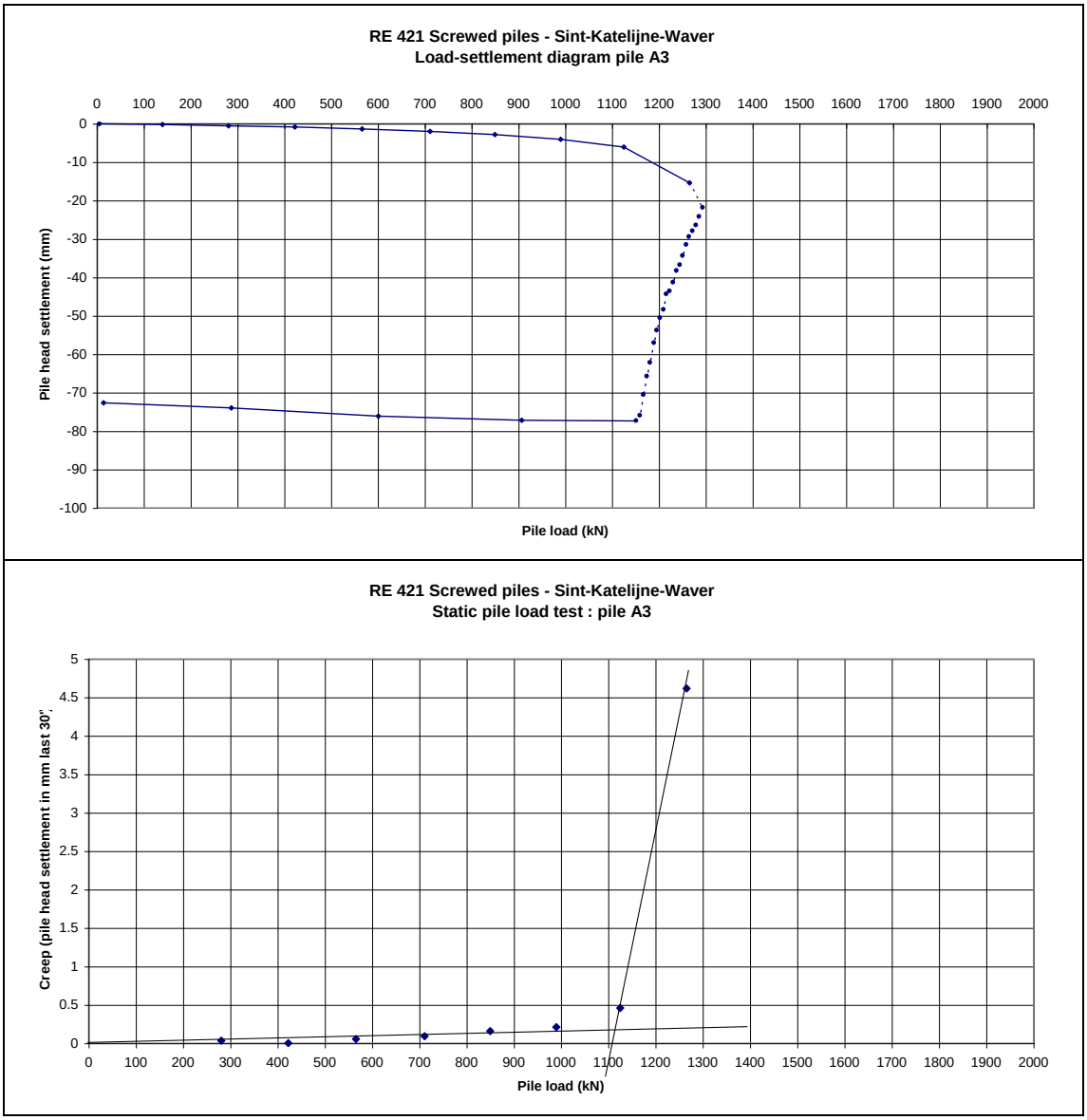

Figure A-3a – Load settlement diagram and creep curve (load vs. $\Delta s_{0\text{-}i,30'}$)
Fundex screw pile A3

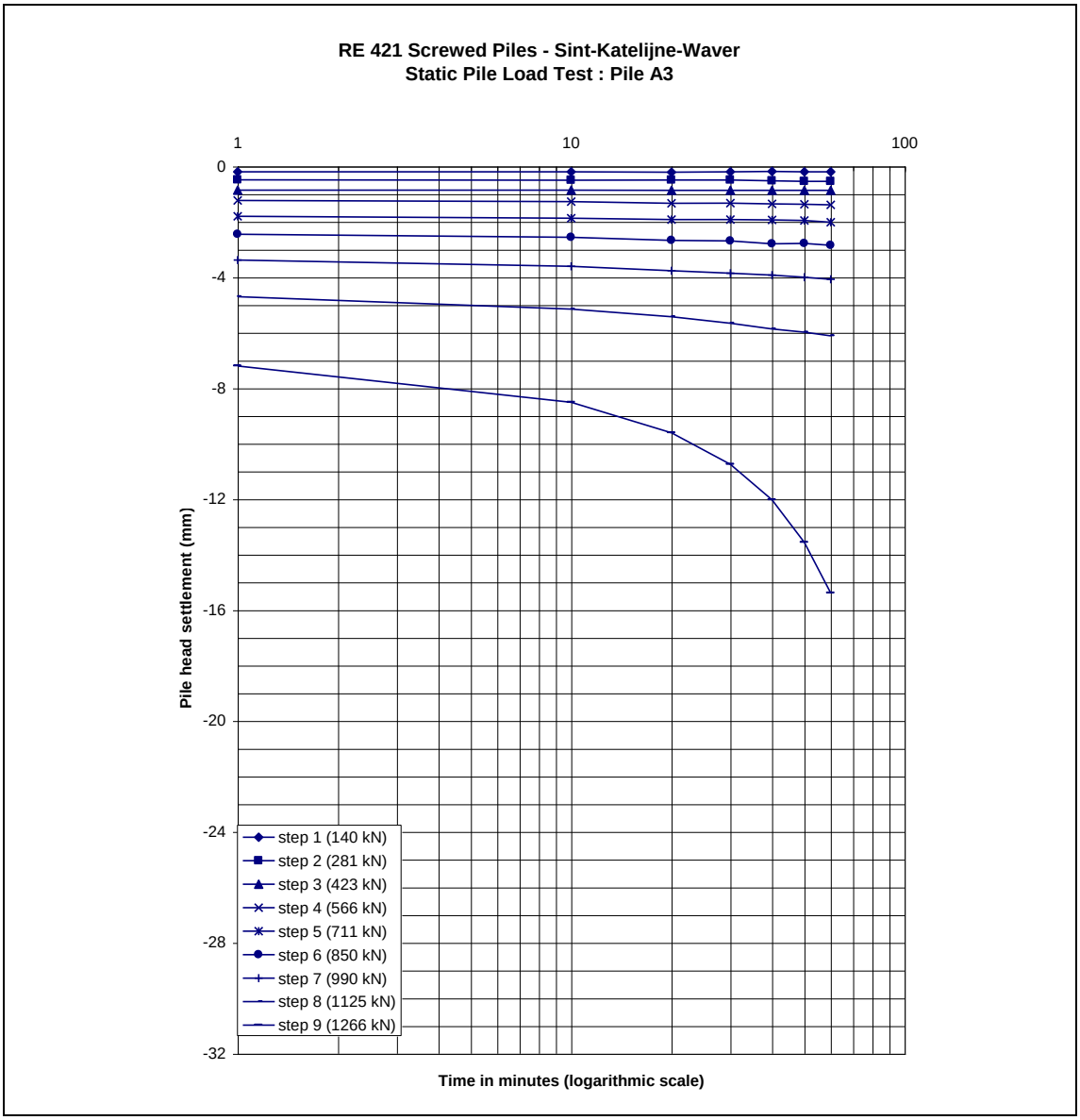

Figure A-3b – Time settlement results for the different (complete) load steps
Fundex screw pile A3

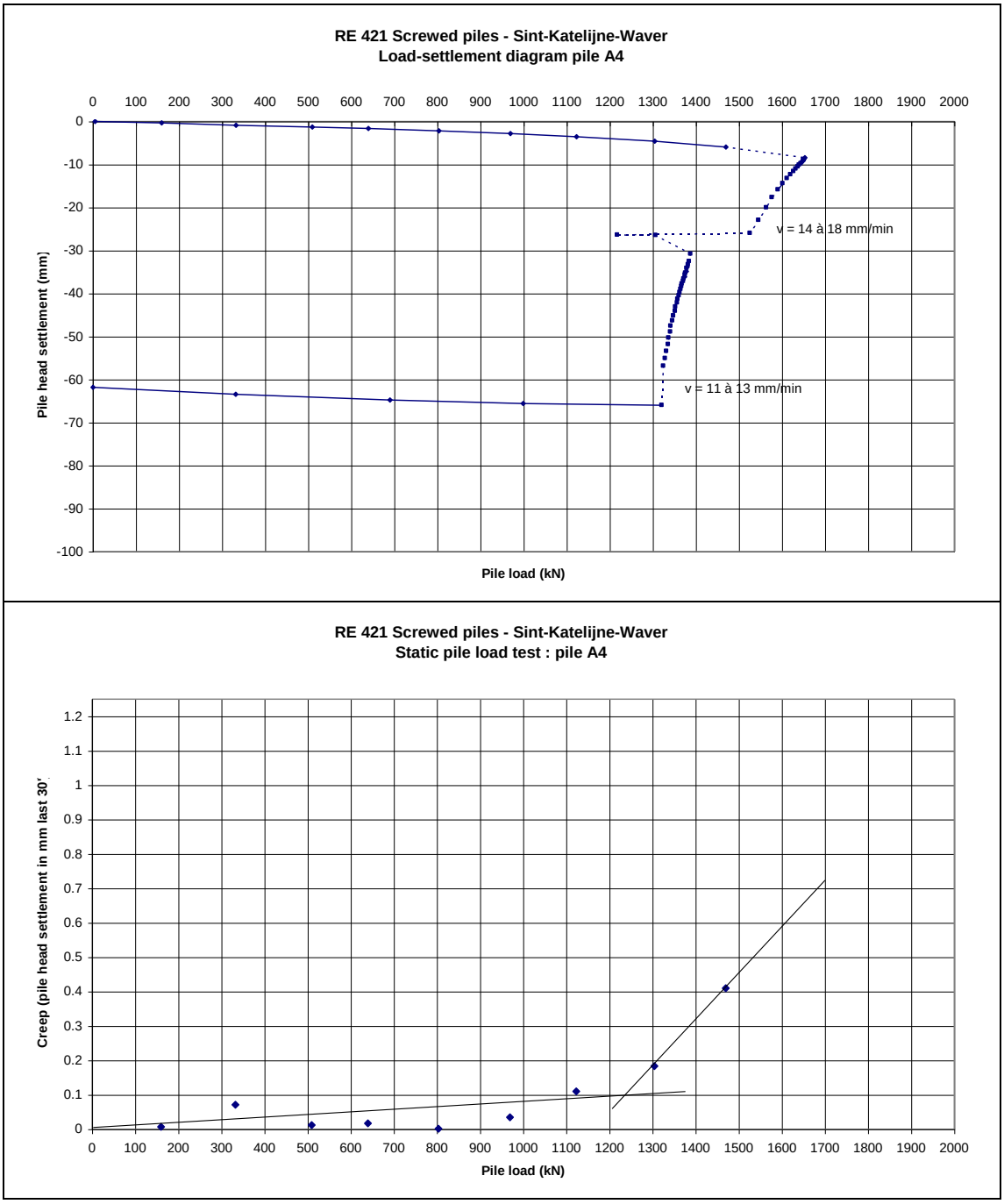

Figure A-4a – Load settlement diagram and creep curve (load vs. $\Delta s_{0\text{-}i,30'}$) driven prefabricated pile A4

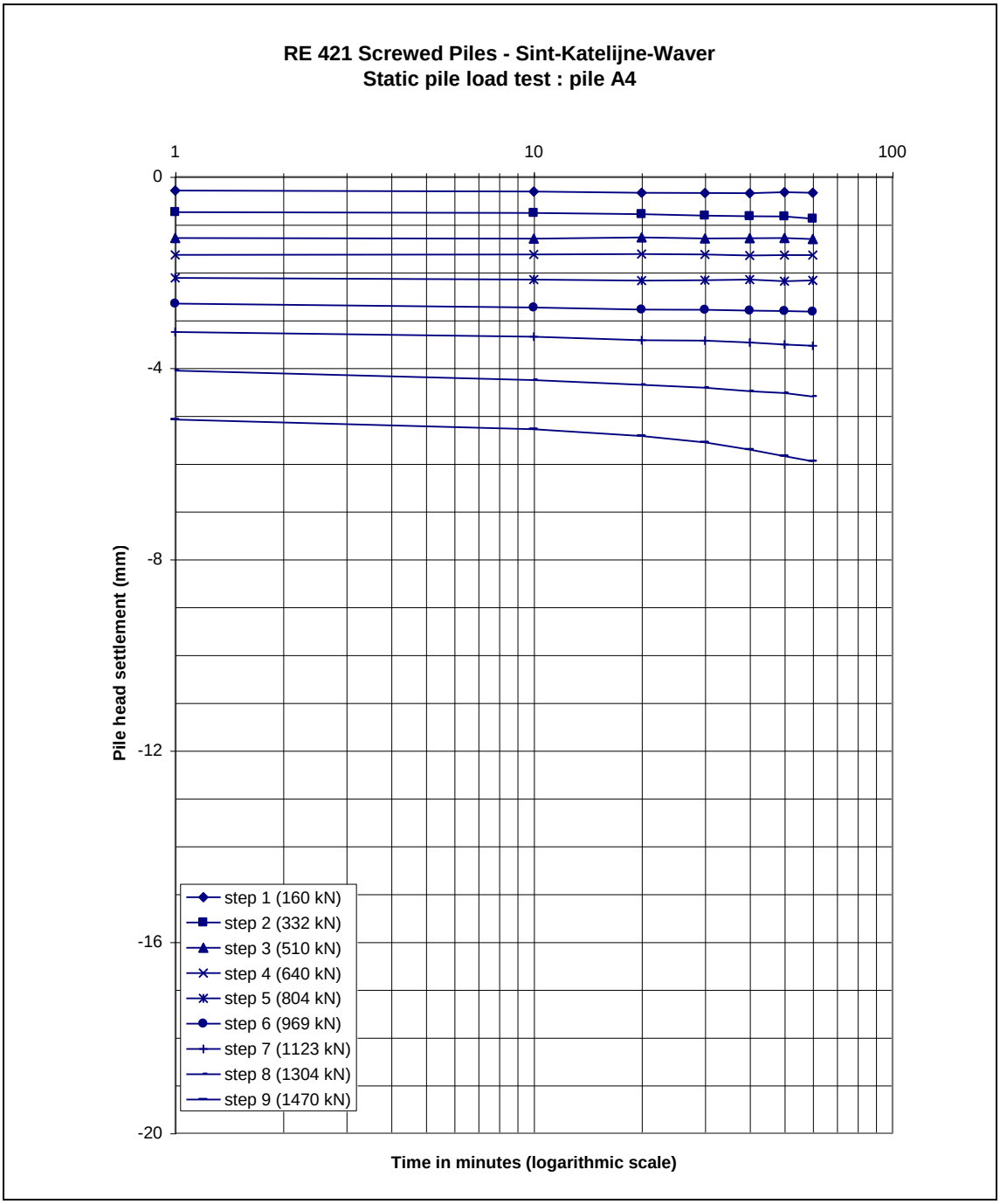

Figure A-4b – Time settlement results for the different (complete) load steps driven prefabricated pile A4

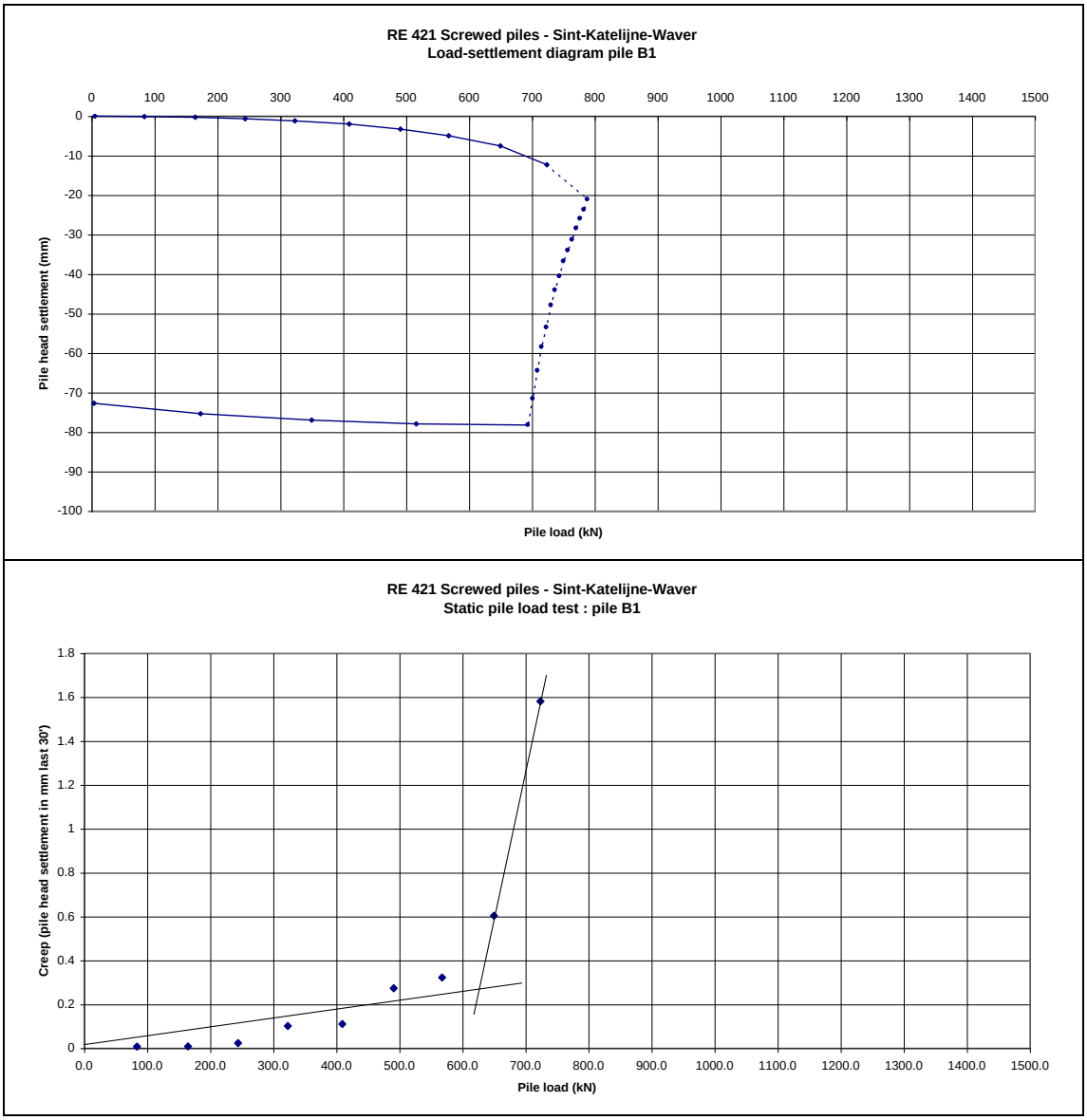

Figure A-5a – Load settlement diagram and creep curve (load vs. $\Delta s_{0\text{-}i,30'}$)
De Waal screw pile B1

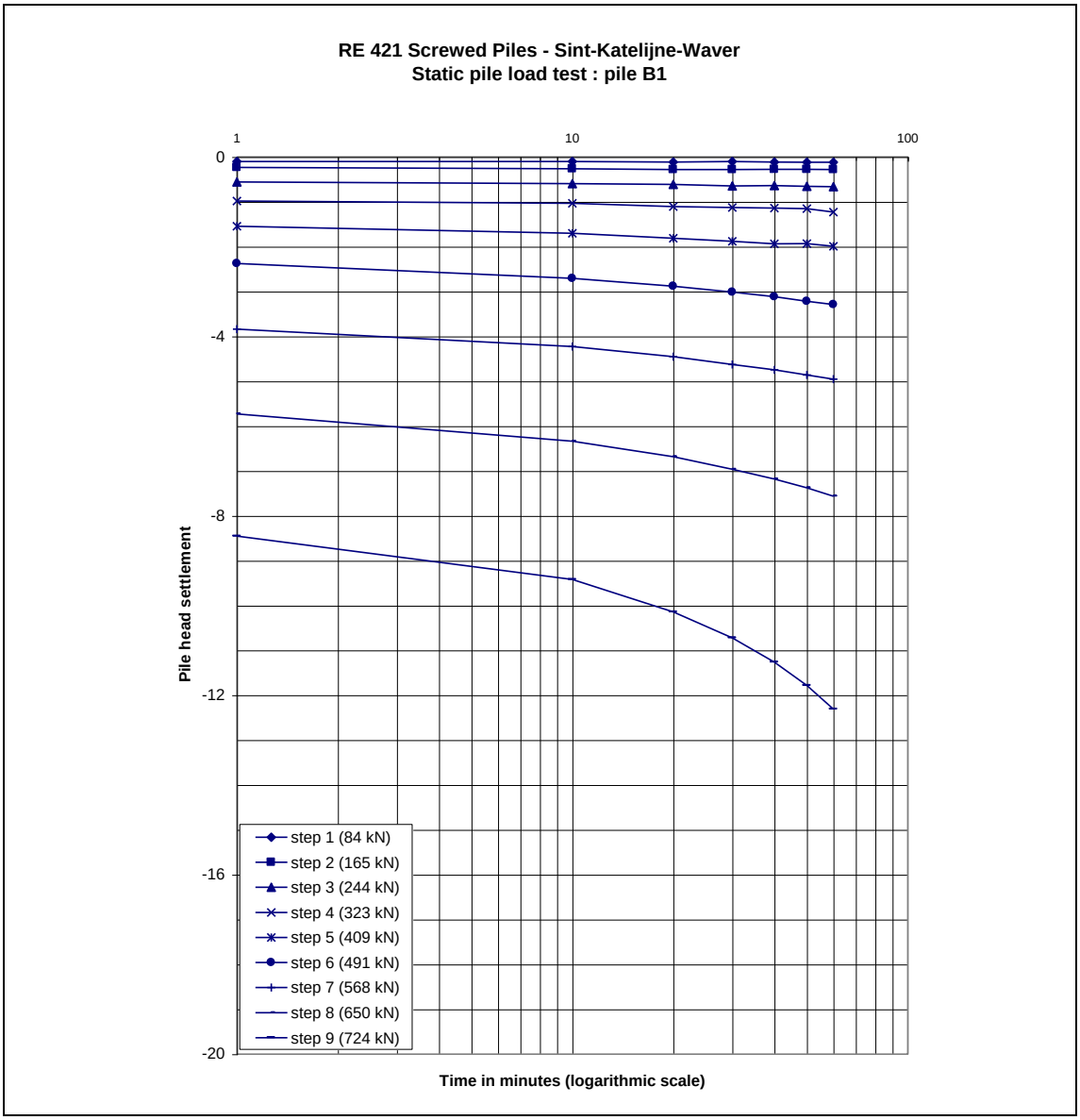

Figure A-5b – Time settlement results for the different (complete) load steps
De Waal screw pile B1

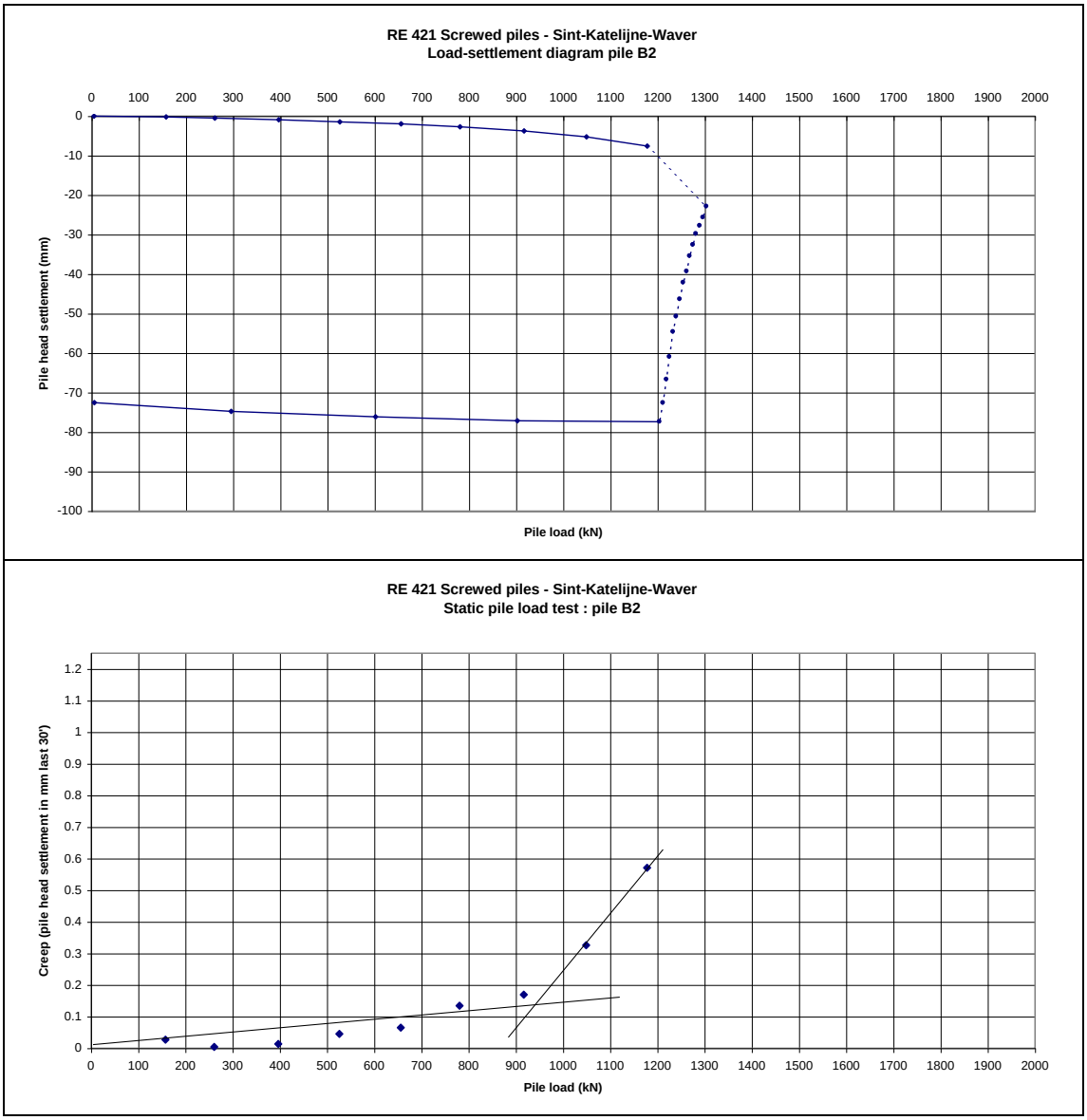

Figure A-6a – Load settlement diagram and creep curve (load vs. $\Delta s_{0\text{-}i,30'}$)
De Waal screw pile B2

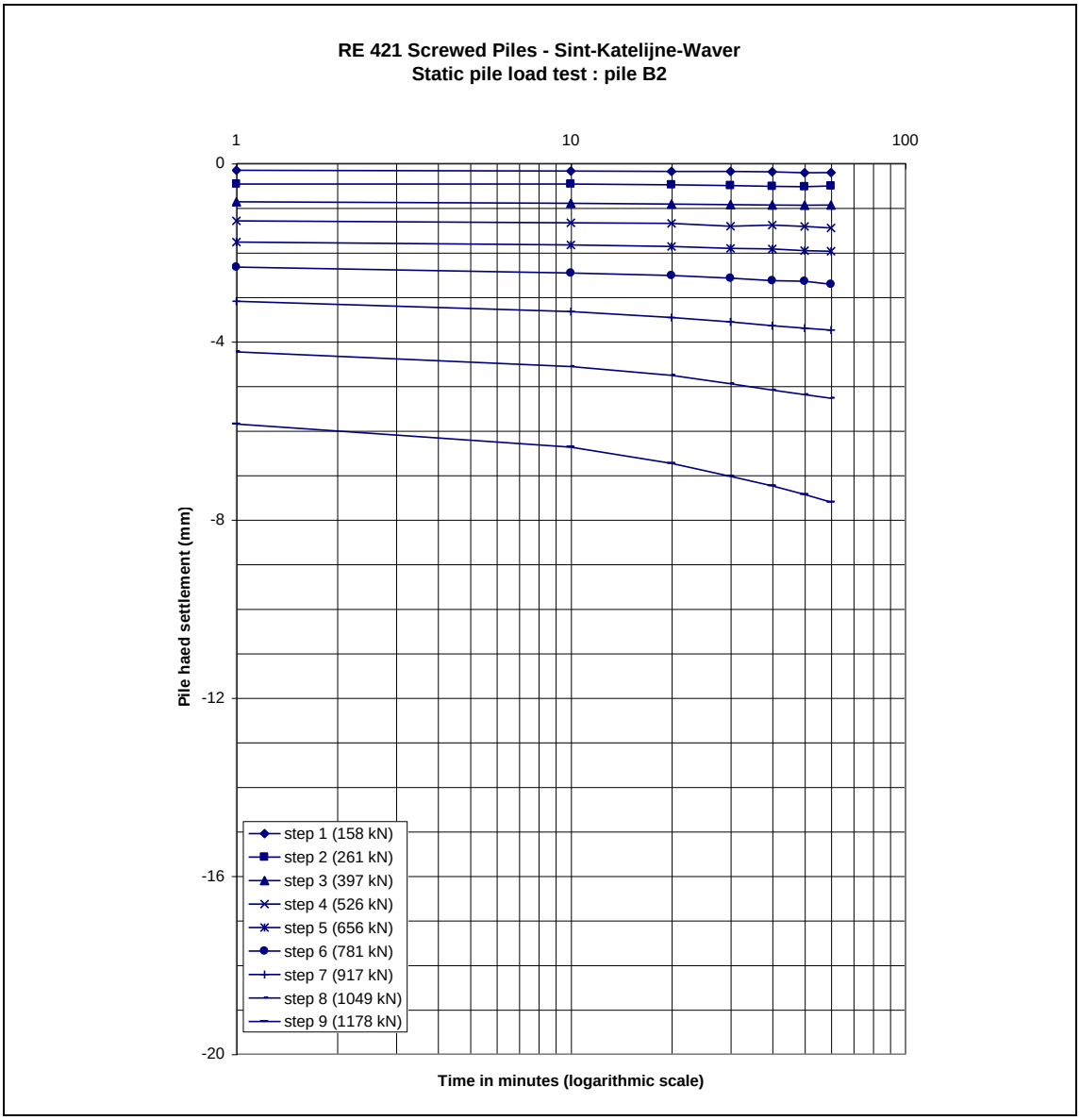

Figure A-6b – Time settlement results for the different (complete) load steps
De Waal screw pile B2

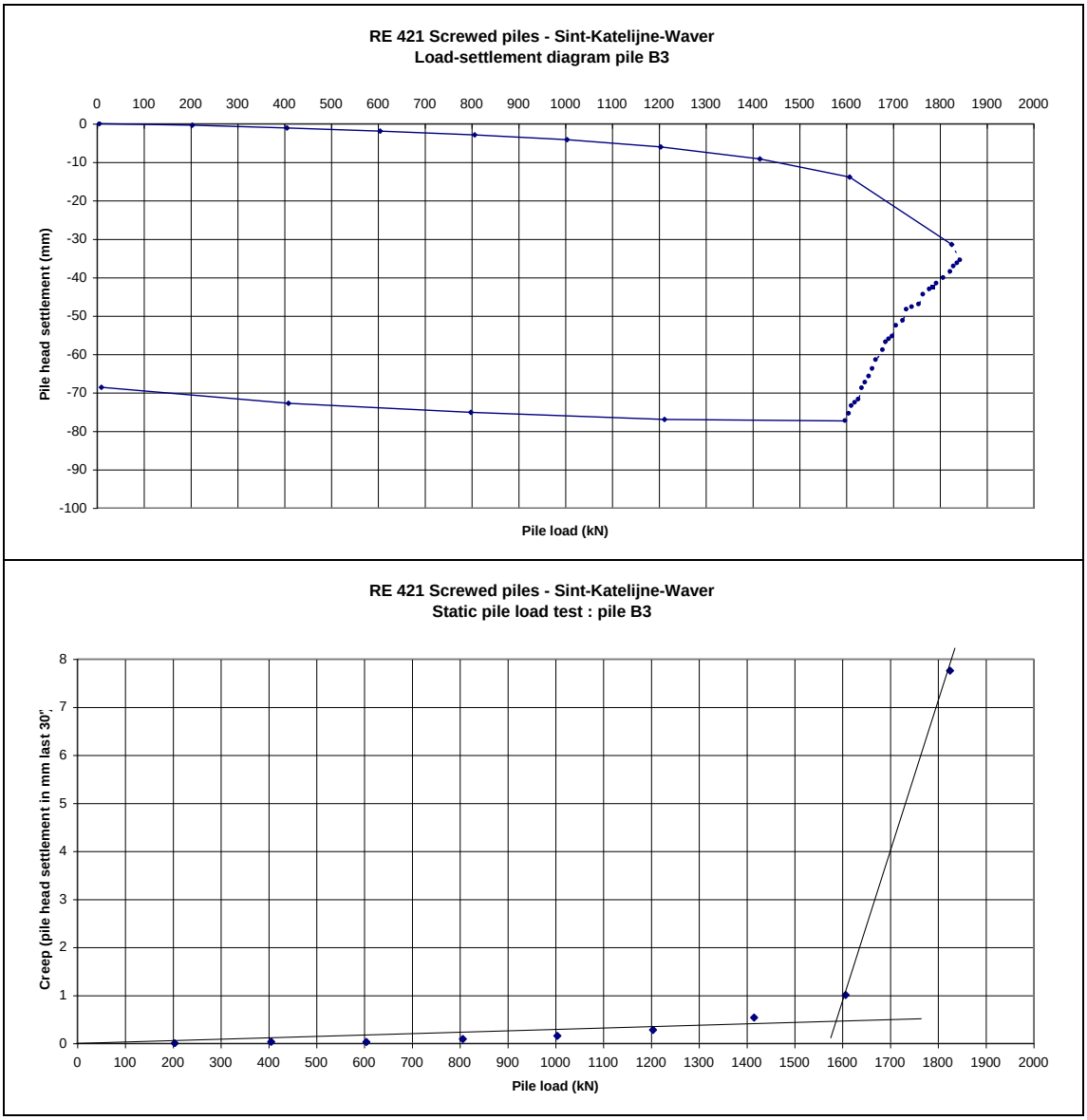

Figure A-7a – Load settlement diagram and creep curve (load vs. $\Delta s_{0\text{-}i,30'}$)
Olivier screw pile B3

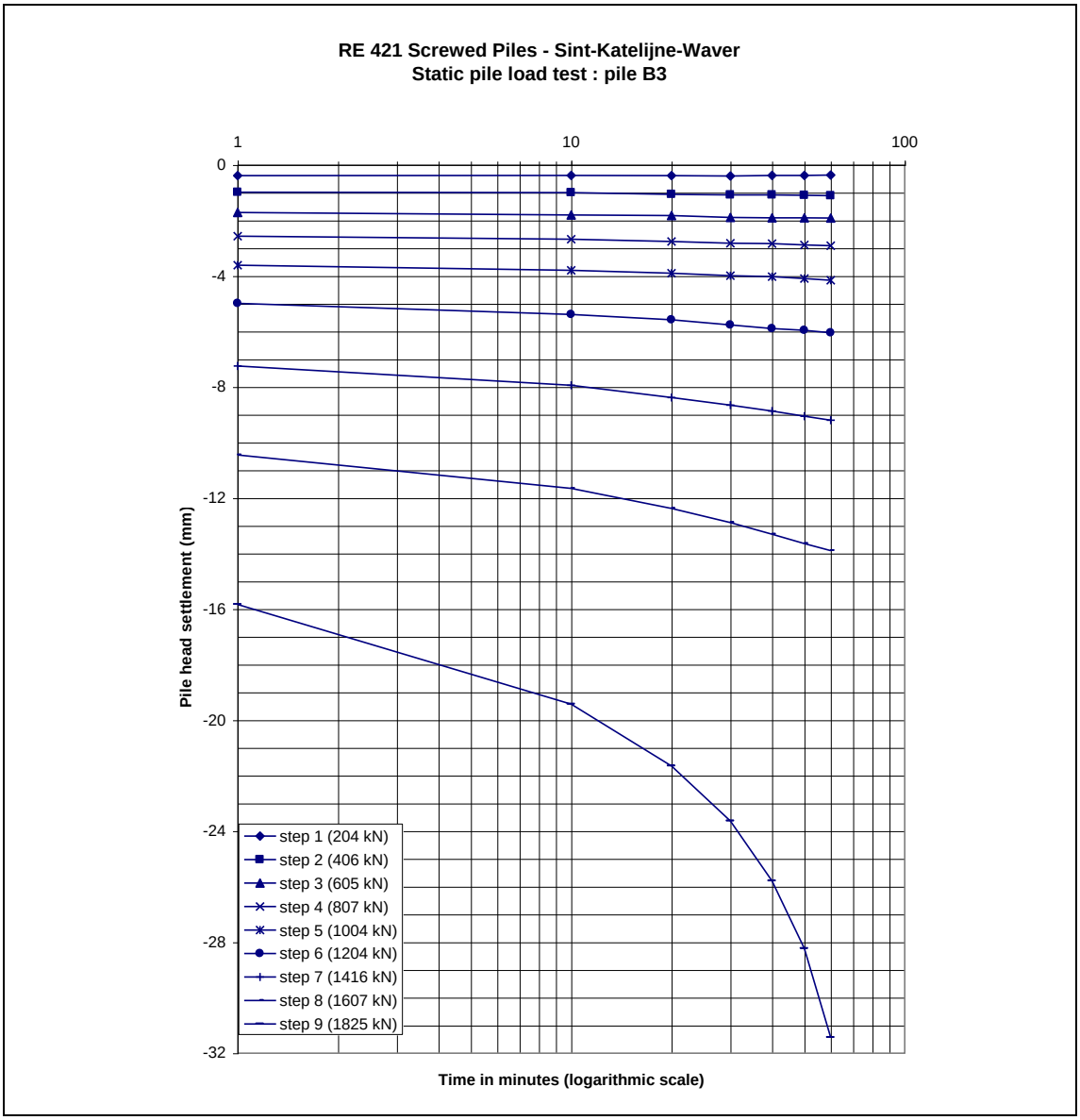

Figure A-7b – Time settlement results for the different (complete) load steps Olivier screw pile B3

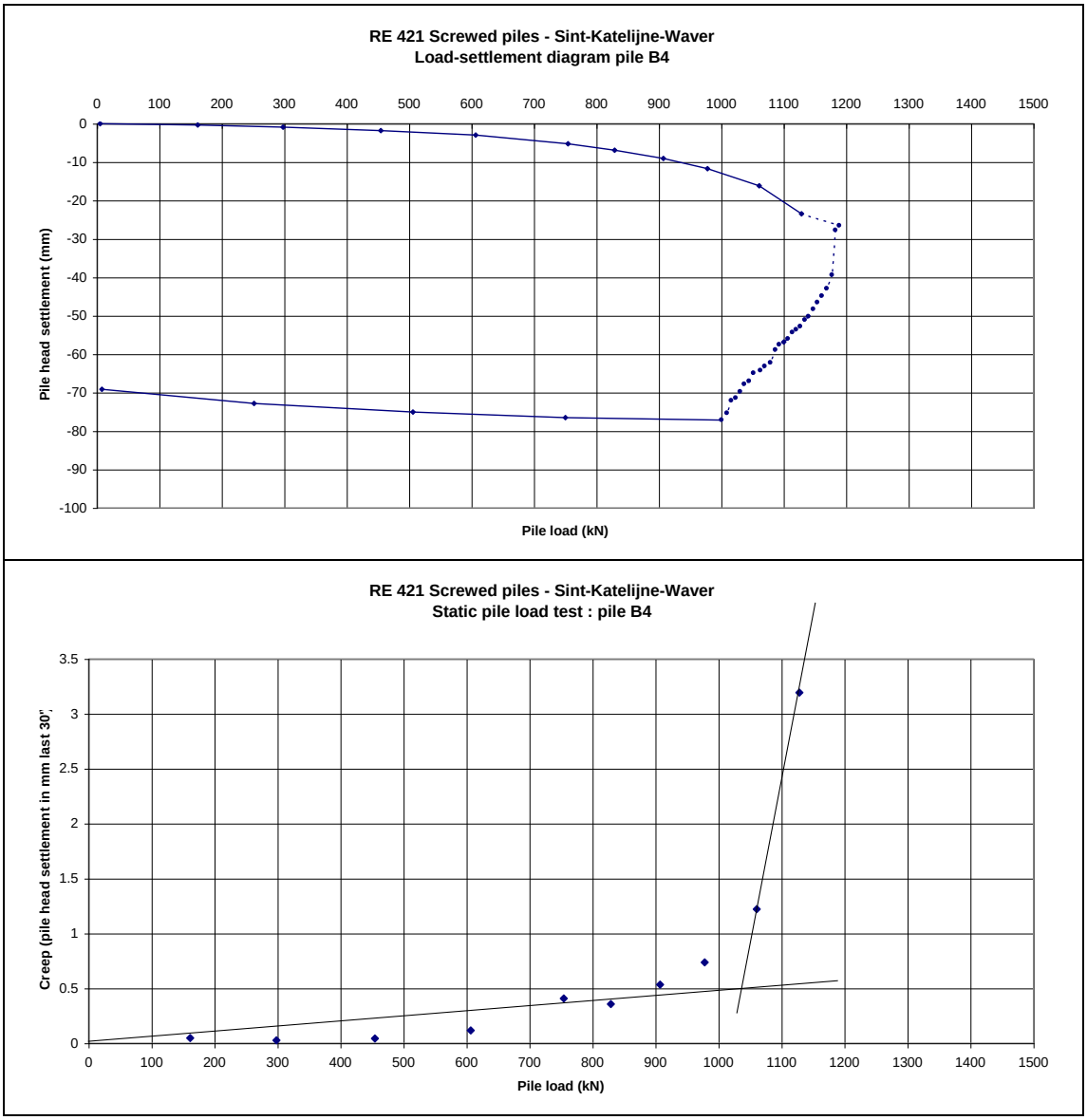

Figure A-8a – Load settlement diagram and creep curve (load vs. $\Delta s_{0\text{-}i,30'}$)
Olivier screw pile B4

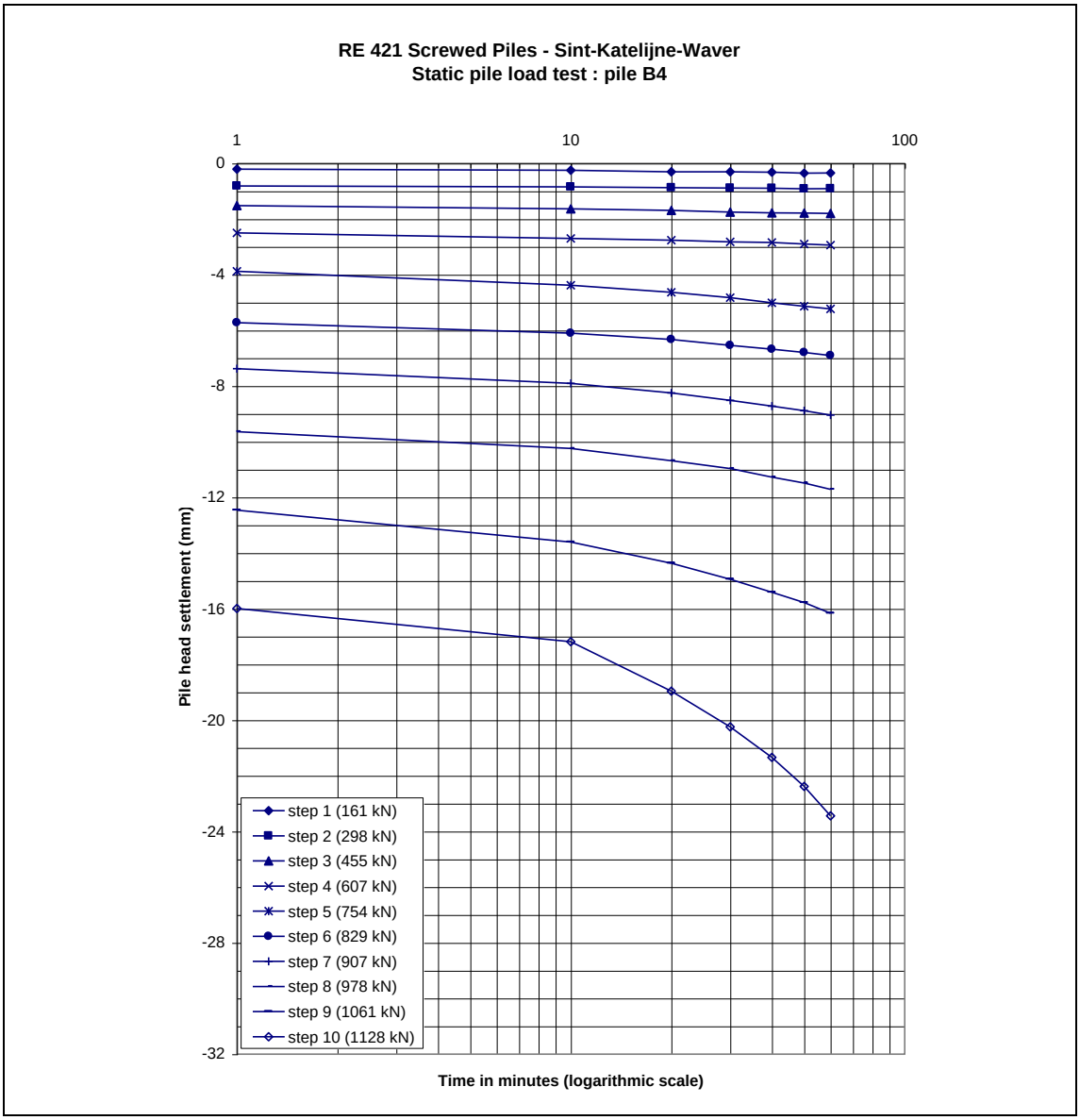

Figure A-8b – Time settlement results for the different (complete) load steps
Olivier screw pile B4

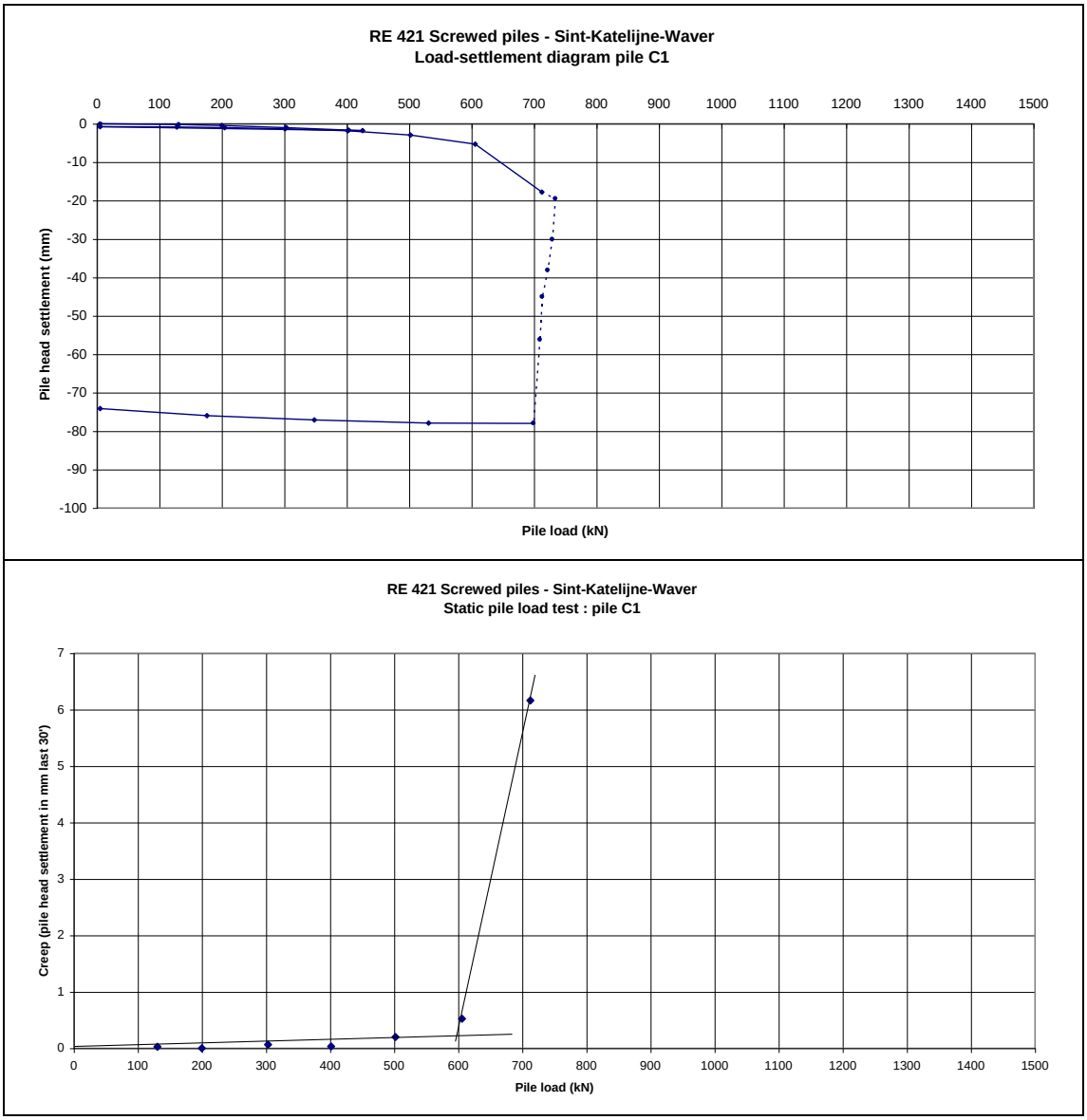

Figure A-9a – Load settlement diagram and creep curve (load vs. $\Delta s_{0\text{-}i,30'}$)
Omega screw pile C1

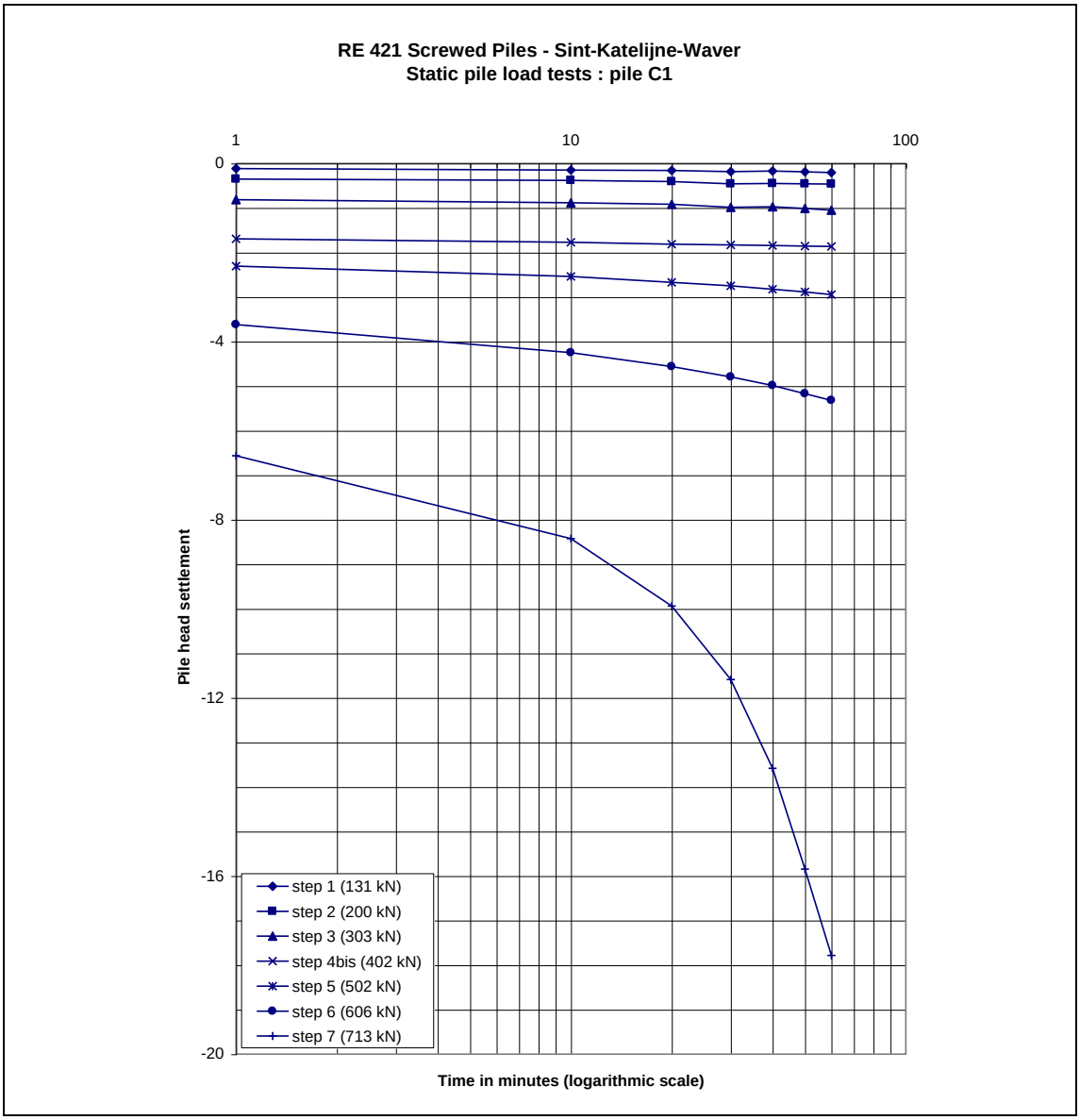

Figure A-9b – Time settlement results for the different (complete) load steps Omega screw pile C1

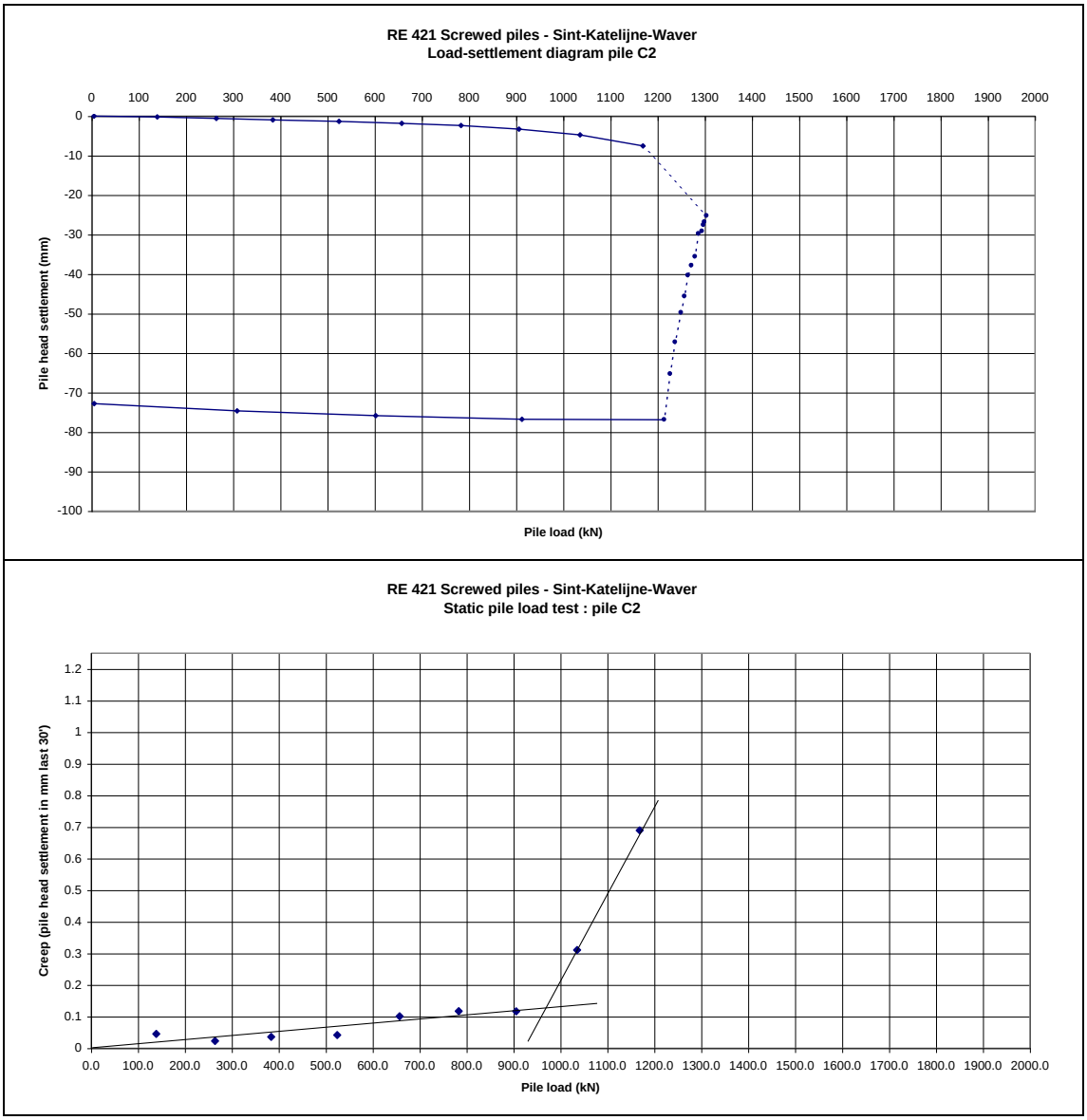

Figure A-10a – Load settlement diagram and creep curve (load vs. $\Delta s_{0\text{-}i,30'}$)
Omega screw pile C2

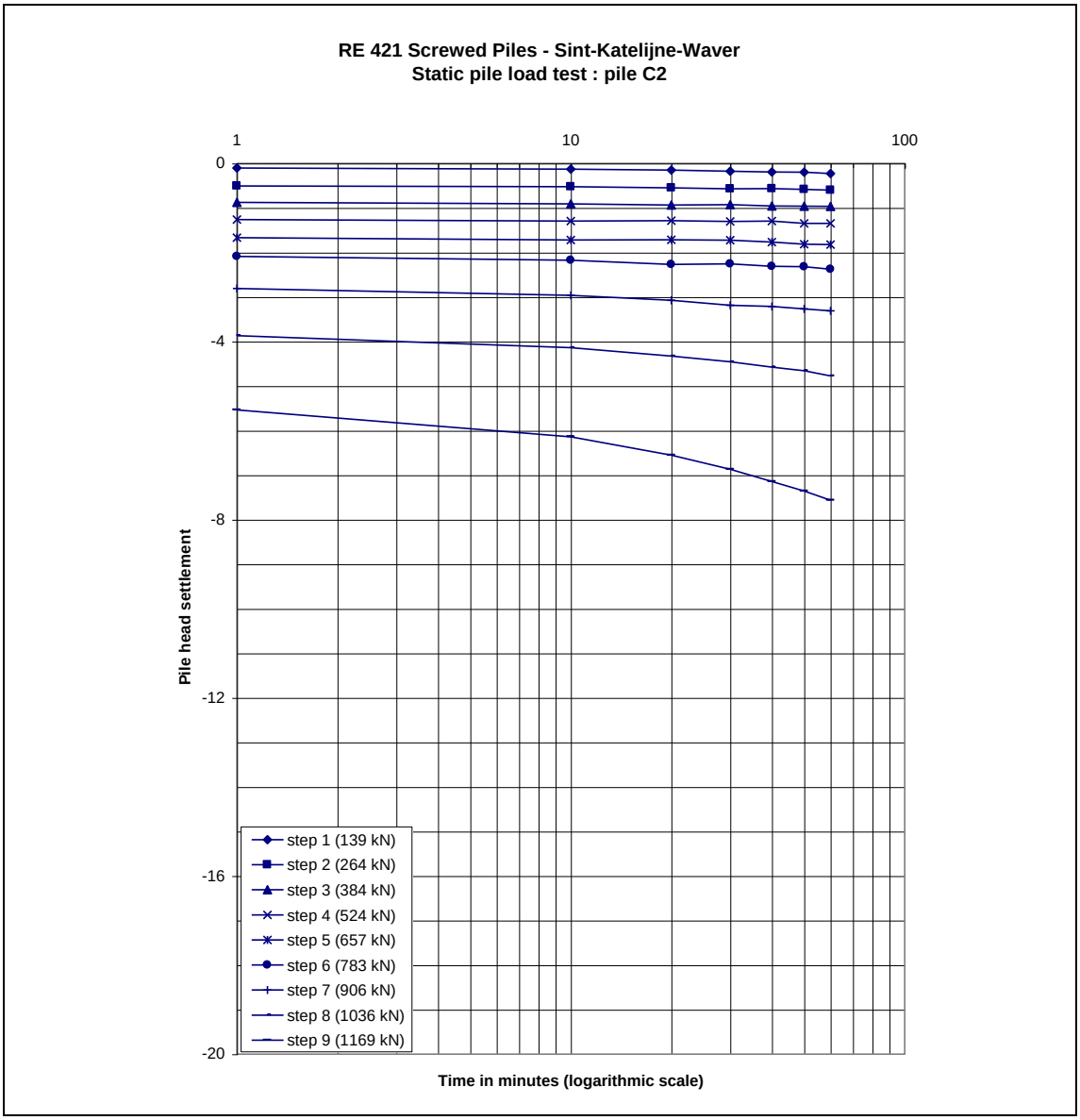

Figure A-10b – Time settlement results for the different (complete) load steps Omega screw pile C2

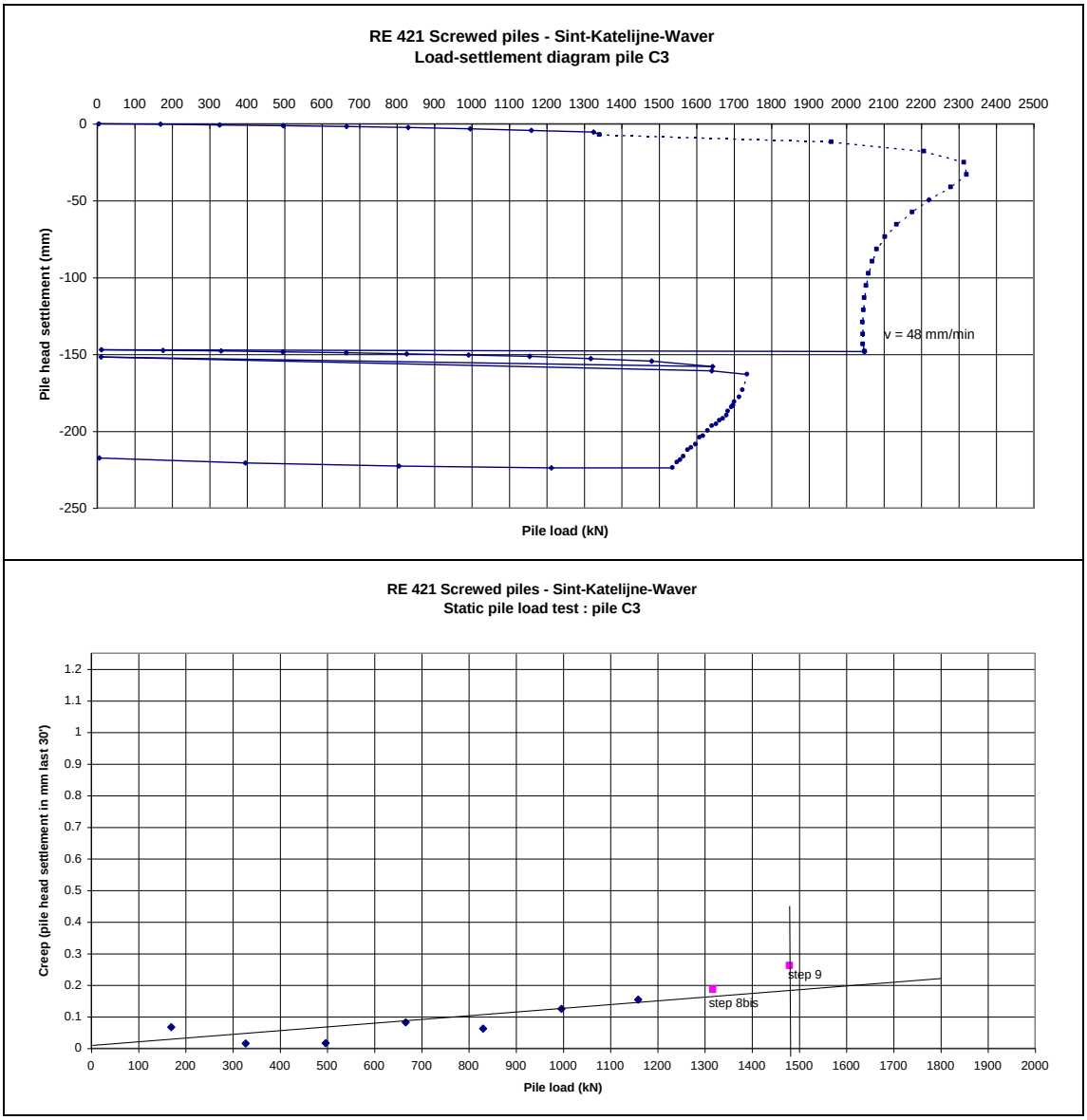

Figure A-11a – Load settlement diagram and creep curve (load vs. $\Delta s_{0\text{-}i,30'}$)
Atlas screw pile C3

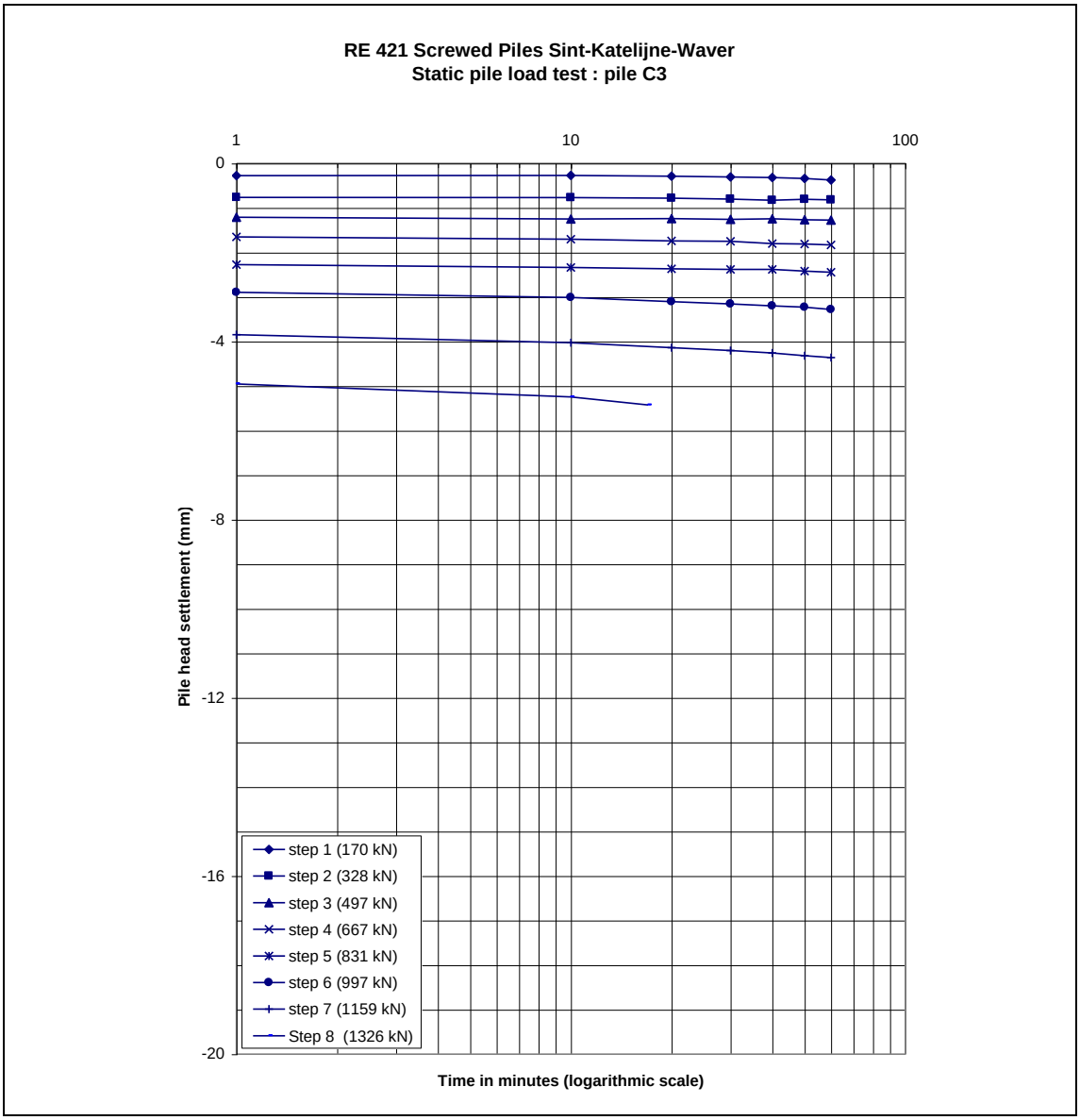

Figure A-11b – Time settlement results for the different load steps (until regulation problem)

Atlas screw pile C3

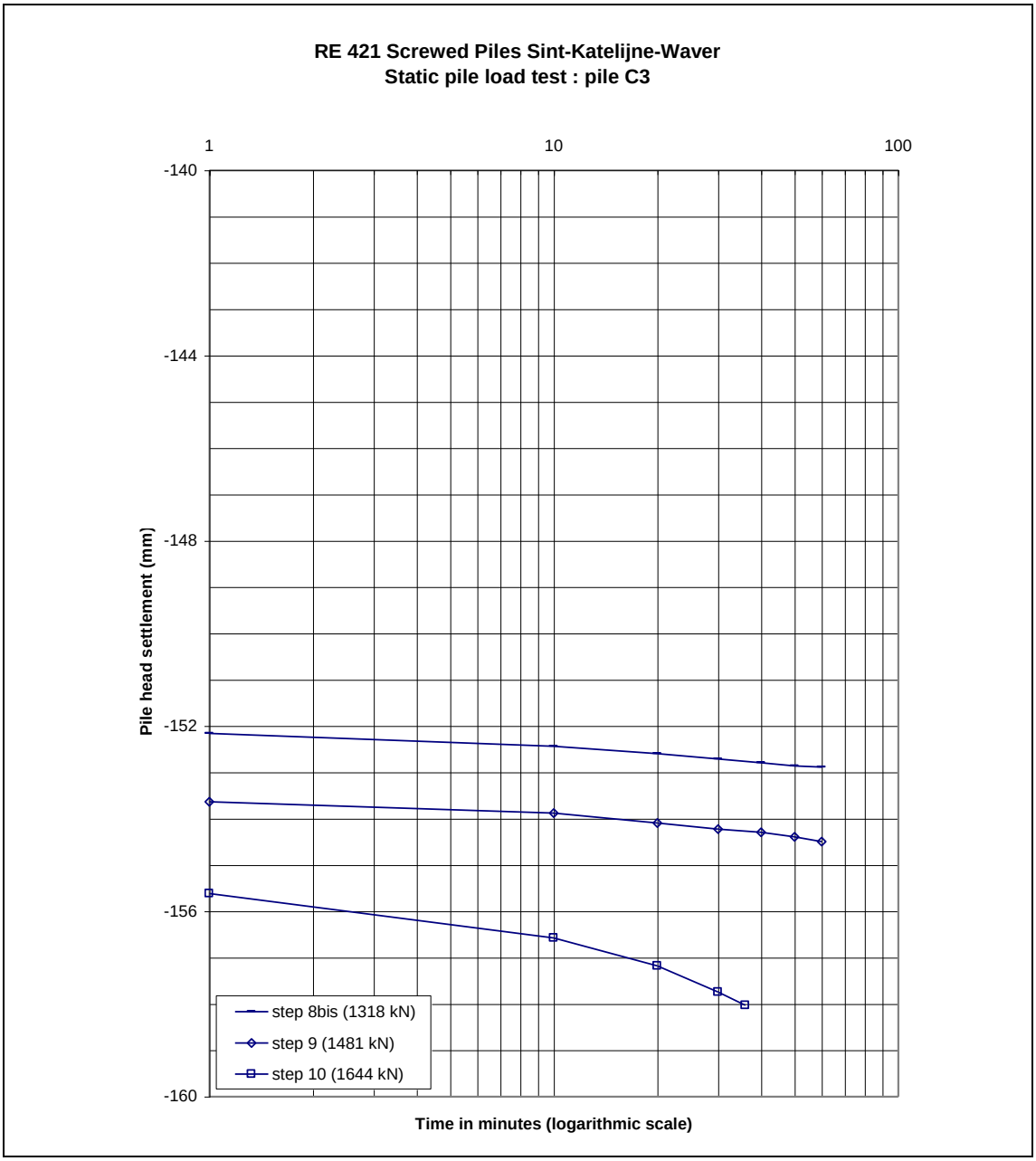

Figure A-11c – Time settlement results for the different load steps (after regulation problem – reloading)

Atlas screw pile C3

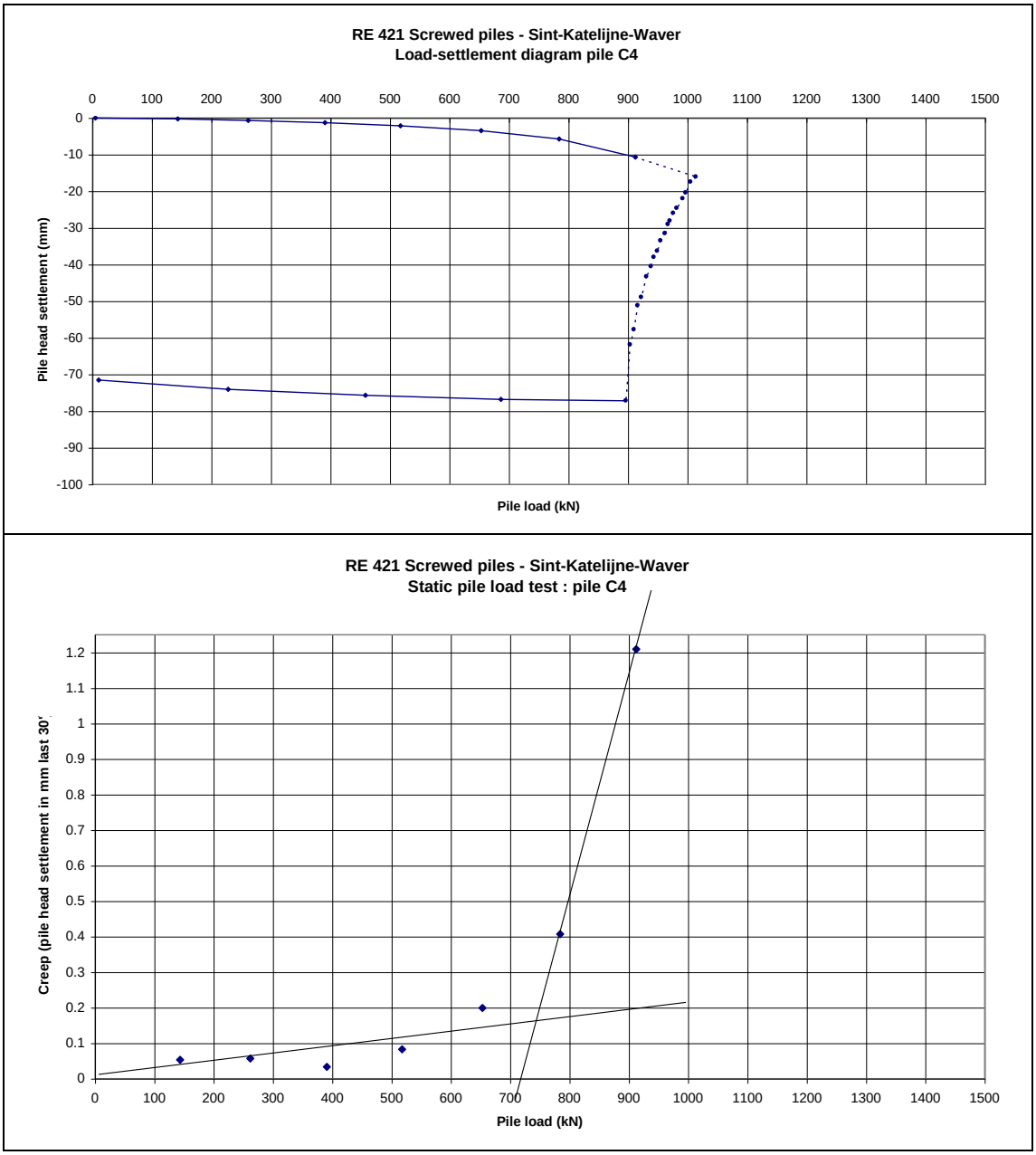

Figure A-12a – Load settlement diagram and creep curve (load vs. $\Delta s_{0\text{-}i,30'}$)
Atlas screw pile C4

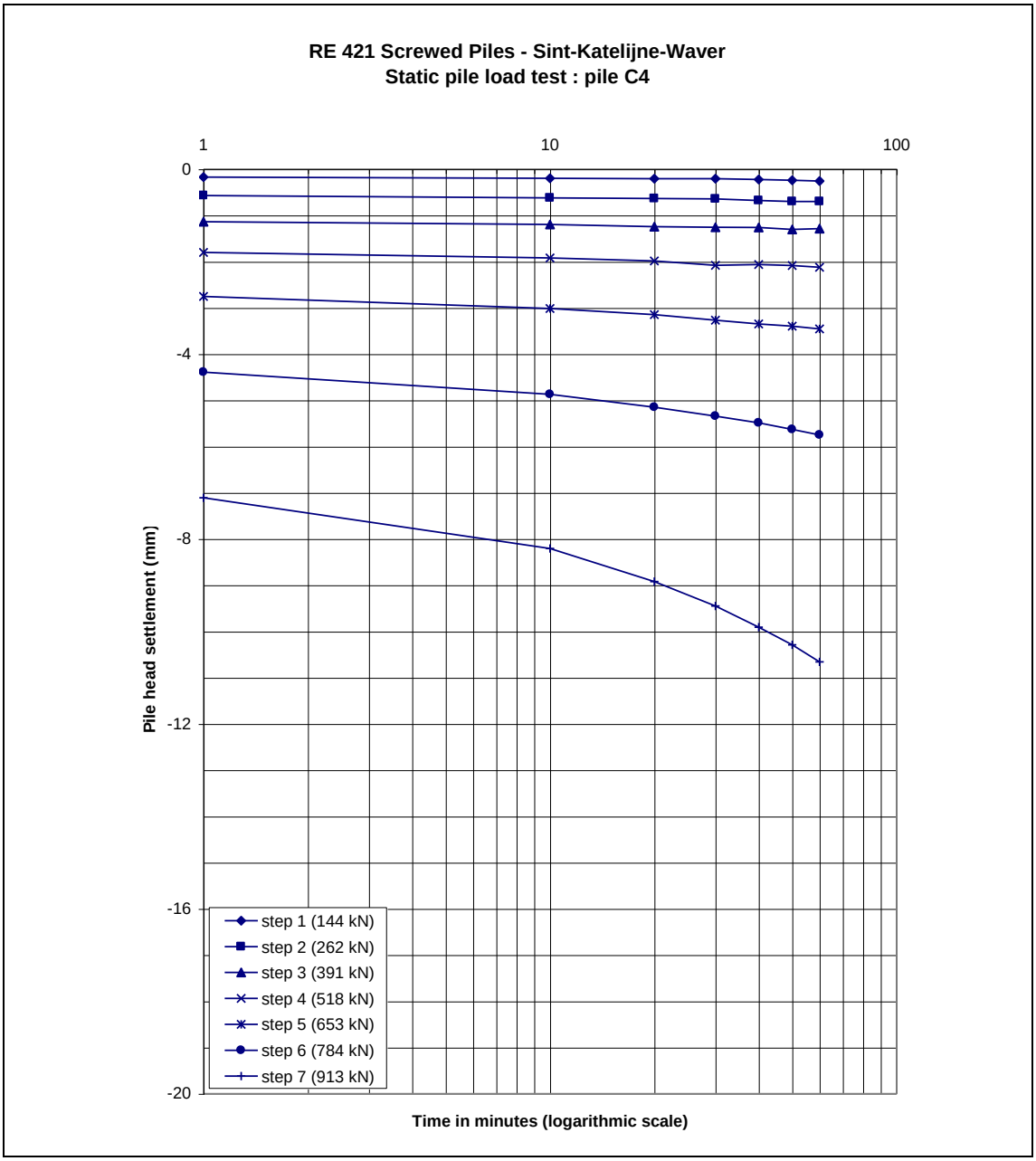

Figure A-12b – Time settlement results for the different (complete) load steps Atlas screw pile C4